AD-A088 917 BELL HELICOPTER TEXTRON FORT WORTH TX F/G 2 /11
INVESTIGATION OF VIBRATION REDUCTION THROUGH STRUCTURAL OPTIMIZ-- TC(U)
JUL 80 H W HANSON DAAK51-78-C-0011
UNCLASSIFIED 699-099-122 USAAVRADCOM-TR-80-D-13 NL

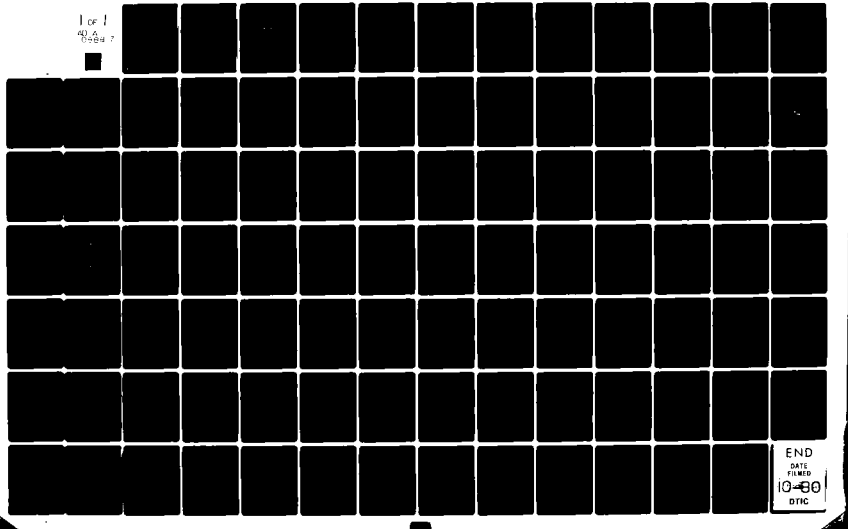

USAAVRADCOM-TR-80-D-13

AD A088917

INVESTIGATION OF VIBRATION REDUCTION THROUGH STRUCTURAL OPTIMIZATION

H. W. Hanson
BELL HELICOPTER TEXTRON
P. O. Box 482
Fort Worth, Tex. 76101

July 1980

Final Report for Period August 1978 - March 1980

Prepared for

APPLIED TECHNOLOGY LABORATORY
U. S. ARMY RESEARCH AND TECHNOLOGY LABORATORIES (AVRADCOM)
Fort Eustis, Va. 23604

APPLIED TECHNOLOGY LABORATORY POSITION STATEMENT

In the area of aircraft structural dynamic design, the existence of a reliable structural optimization method can be a valuable design tool, enabling a designer to perform rapid identification and evaluation of the most promising structural elements, which, upon modification of their modal properties, could minimize vibration response. In this program, a feasibility study was performed to evaluate two structural optimization methods, the Vincent circle and the forced response strain energy method for reducing vibration response, primarily via structural stiffness changes, using NASTRAN beam-element representation of the AH-1G with uniform damping. The forcing function consisted of a single main rotor 2 rev steady-state vertical excitation. The pilot's seat was selected as the location for dynamic response reduction.

The relative effectiveness of the methods to minimize the dynamic response at the selected location, subject to the constraints and considerations stated above, was based essentially on two factors: (a) selection of practical stiffness changes that an element can undergo, and (b) evaluation of the effectiveness of the groups of elements predicted by each method by calculating the response of the structure subject to practical stiffness changes.

The results obtained from the two methods, i.e., stiffness changes required and group of elements identified with high potential for reducing vibration, at best, do not agree. These results indicate that the forced response strain energy method is more suitable in attaining response reduction according to the investigative methodology used in this program.

The Vincent circle method was further investigated in conjunction with mass and damping changes. Also, the possibility that the Vincent circle method would indicate the optimum location of a fixed mass and damping dynamic absorber was investigated, yielding negative results.

The project engineer for this effort was Mr. N. J. Calapodas of the Aeronautical Technology Division, Structures Technical Area.

DISCLAIMER NOTICE

THIS DOCUMENT IS BEST QUALITY PRACTICABLE. THE COPY FURNISHED TO DTIC CONTAINED A SIGNIFICANT NUMBER OF PAGES WHICH DO NOT REPRODUCE LEGIBLY.

UNCLASSIFIED

SECURITY CLASSIFICATION OF THIS PAGE (When Data Entered)

REPORT DOCUMENTATION PAGE	READ INSTRUCTIONS BEFORE COMPLETING FORM
1. REPORT NUMBER: USAAVRADCOM TR-80-D-13	2. GOVT ACCESSION NO.: AD-A088917
3. RECIPIENT'S CATALOG NUMBER	
4. TITLE (and Subtitle): INVESTIGATION OF VIBRATION REDUCTION THROUGH STRUCTURAL OPTIMIZATION	5. TYPE OF REPORT & PERIOD COVERED: Final Report, August 1978 — March 1980
6. PERFORMING ORG. REPORT NUMBER: 699-099-122	
7. AUTHOR(s): Horace W. Hanson	8. CONTRACT OR GRANT NUMBER(s): DAAK51-78-C-0011
9. PERFORMING ORGANIZATION NAME AND ADDRESS: Bell Helicopter Textron, P.O. Box 482, Fort Worth, Texas 76101	10. PROGRAM ELEMENT, PROJECT, TASK AREA & WORK UNIT NUMBERS: 62209A 1L162209AH76 00 249 EK
11. CONTROLLING OFFICE NAME AND ADDRESS: Applied Technology Laboratory, U.S. Army Research & Technology Laboratories (AVRADCOM), Fort Eustis, Virginia 23604	12. REPORT DATE: July 1980
	13. NUMBER OF PAGES: 93
14. MONITORING AGENCY NAME & ADDRESS (if different from Controlling Office)	15. SECURITY CLASS. (of this report): Unclassified
	15a. DECLASSIFICATION/DOWNGRADING SCHEDULE

16. DISTRIBUTION STATEMENT (of this Report)

Approved for public release; distribution unlimited.

17. DISTRIBUTION STATEMENT (of the abstract entered in Block 20, if different from Report)

18. SUPPLEMENTARY NOTES

19. KEY WORDS (Continue on reverse side if necessary and identify by block number)

Helicopter	Optimization	Forced response
Dynamic	Vincent circle	Modal
Vibration	NASTRAN	
Structure	Strain energy	

20. ABSTRACT (Continue on reverse side if necessary and identify by block number)

The purpose of this program was to investigate structural optimization techniques for vibration reduction. The results of a practical evaluation of two such techniques, the Vincent circle method and the forced response strain energy method, are discussed. Initial comparison studies of the two methods based on stiffness parameter variations were conducted using an elastic-line NASTRAN

(continued)

DD FORM 1 JAN 73 1473 EDITION OF 1 NOV 65 IS OBSOLETE

UNCLASSIFIED

SECURITY CLASSIFICATION OF THIS PAGE (When Data Entered)

054200

model of the AH-1G helicopter. The forced response strain energy method was then applied to a large complex built-up NASTRAN AH-1G model. This application provided useful comparative data identifying the structural elements considered to be the primary contributors to the response. Realistic structural stiffness changes in these elements were assessed to determine their effect on vibration reduction. The Vincent circle method was further evaluated for mass tuning, damping, and dynamic absorber parameters using the elastic-line model.

PREFACE

This investigation of vibration reduction through structural optimization was performed under Contract DAAK51-78-C-0011 for the Applied Technology Laboratory, U. S. Army Research and Technology Laboratories (AVRADCOM), Fort Eustis, Virginia. The program was implemented under the technical direction of Mr. Nicholas J. Calapodas of the Applied Technology Laboratory.

A literature survey of structural optimization techniques for vibration reduction was performed and two techniques - the Vincent circle method and the forced response strain energy method - were evaluated using a NASTRAN analysis of the Model AH-1G helicopter. Mr. Horace W. Hanson was the Bell Helicopter Textron Project Engineer.

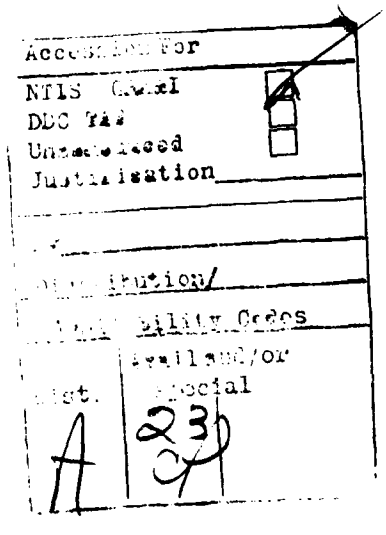

TABLE OF CONTENTS

LIST OF ILLUSTRATIONS

LIST OF ILLUSTRATIONS - Concluded

LIST OF TABLES

INTRODUCTION

In the development of a helicopter airframe structure, part of the design cycle must be concerned with keeping vibration to a minimum. The analysis and control of helicopter airframe dynamic characteristics are quite complex. The reasons are, in part:

- The large number of main rotor harmonic excitations simultaneously present, as well as excitations from secondary sources such as the tail rotor and shafting.

- The large variation in main rotor oscillatory hub forces and moments and phase relationships as a function of ship gross weight and center-of-gravity, airspeed, temperature, altitude, etc.

- The large number of locations at which vibrations must be controlled within the aircraft for reasons of crew and passenger comfort, system reliability, and service life of the airframe structure and components.

- Design changes for vibration control that must be accomplished within the framework of the overall design criteria, including many considerations such as size, strength, weight, and aerodynamic drag.

Vibration reduction is primarily accomplished through dynamic devices such as vibration isolation systems and dynamic absorbers, and/or through structural modifications that improve the vibratory elastic deformation characteristics of the airframe. Rapid and efficient techniques are needed for evaluating and optimizing these structural changes to minimize the vibration response. Two methods of reducing vibration through structural optimization were evaluated in this study - the Vincent circle method and the forced response strain energy method.

LITERATURE SURVEY

A brief search was conducted to locate and review existing literature applicable to vibration reduction by structural optimization techniques with emphasis on the Vincent circle and the forced response strain energy methods. Three data bases were used in the survey:

- The National Technical Information Service (NTIS)
- The Defense Technical Information Center (DTIC)
- The Engineering Index (COMPENDEX)

The information that is cataloged in the National Technical Information Service is derived from publications of the federal, state, and local government agencies; private industry; and universities, with emphasis placed on commercial applications. The information available from DTIC is obtained from many of the same sources as NTIS; however, the emphasis is placed on military and defense usage. The Engineering Index contains publications of the engineering societies, such as the proceedings of conferences, journals, and magazines.

Five documents applicable to the Vincent circle method were found (References 1 through 5). Only one report addressing

---

[1]Vincent, A. H., A NOTE ON THE PROPERTIES OF THE VARIATION OF STRUCTURAL RESPONSE WITH RESPECT TO A SINGLE STRUCTURAL PARAMETER WHEN PLOTTED IN THE COMPLEX PLANE, Westland Helicopters Limited Report GEN/DYN/RES/010R, Yeovil, Somerset, England, September 1973.

[2]Done, G. T. S., and Hughes. A. D., THE RESPONSE OF A VIBRATING STRUCTURE AS A FUNCTION OF STRUCTURAL PARAMETERS, Journal of Sound and Vibration, Vol. 38, No. 2, 1975, pp. 255-266.

[3]Done, G. T. S., and Hughes, A. D., REDUCING VIBRATION BY STRUCTURAL MODIFICATION, Vertica, Vol. 1, No. 1, 1976, pp. 31-38, (paper presented at the First European Rotorcraft and Powered Lift Aircraft Forum at Southampton, September 22-24, 1975).

[4]Done, G. T. S., Hughes, A. D., and Webby, J., THE RESPONSE OF A VIBRATING STRUCTURE AS A FUNCTION OF STRUCTURAL PARAMETERS - APPLICATION AND EXPERIMENT, Journal of Sound and Vibration, Vol. 49, No. 2, 1976, pp. 149-159.

[5]Balmford, D. E. H., THE CONTROL OF VIBRATION IN HELICOPTERS, Aeronautical Journal, Vol. 81, No. 794, February 1977, pp. 63-67.

the forced response strain energy method was located (Reference 6).

The search did not disclose any other literature that dealt specifically with vibration reduction through structural optimization.

---

[6]Sciarra, J. J., USE OF THE FINITE ELEMENT DAMPED FORCED RESPONSE STRAIN ENERGY DISTRIBUTION FOR VIBRATION REDUCTION, Boeing-Vertol Company Report D210-10819-1, U.S. Army Research Office - Durham, Durham, North Carolina, July, 1974.

STRUCTURAL OPTIMIZATION METHODS UNDER EVALUATION

VINCENT CIRCLE METHOD

If a damped linear structure is excited by a constant sinusoidal force at a single location, the response of some other point in the structure can be shown to trace out a circular locus in the complex plane when any single structural element stiffness or mass parameter is continuously varied from minus infinity to plus infinity, as illustrated in Figure 1. This dynamic property of linear structures is known as the Vincent circle phenomenon (Reference 1). The phenomenon requires that some value of damping be present in order to develop the imaginary component of the response. The minimum response attainable, due to a particular stiffness or mass parameter, is indicated by the radius of the response circle and location of its center. Use of these circular properties will hereafter be referred to as the Vincent circle method.

The relevant mathematics of this circular response phenomenon, based on the theory originally established by Vincent, are given by Done and Hughes (Reference 2) and are summarized as follows:

The structure shown in Figure 1 has many degrees-of-freedom, and the response at point q due to a single sinusoidal force at point p is being examined. The amplitude of the displacement response vector, x, for the structure is given by

$$x = GF \tag{1}$$

where

$$G = \tilde{[K - M\omega^2 + i\omega C]}^{-1} \tag{2}$$

Consider two points, r and s, in the structure having mutually compatible degrees of freedom. A linear spring of stiffness, k, is inserted between these two points so as to exert zero force when the original structure is in equilibrium. Considering the structure as a free body, the forces exerted on it at points r and s by the spring are F_r and F_s, respectively, which have the relationship

$$F_r = k(x_s - x_r) = -F_s \tag{3}$$

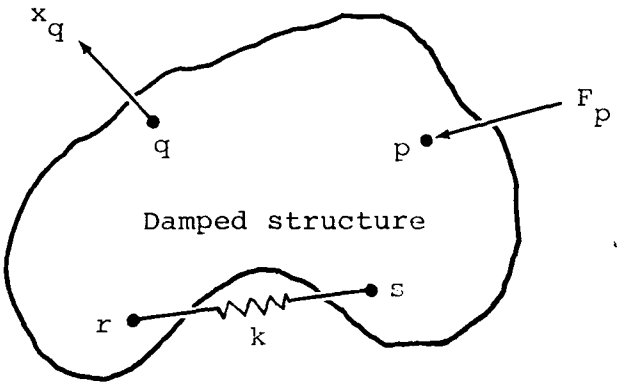

Apply constant sinusoidal force of amplitude F at point p, vary spring stiffness k between points r and s, and measure response x at point q.

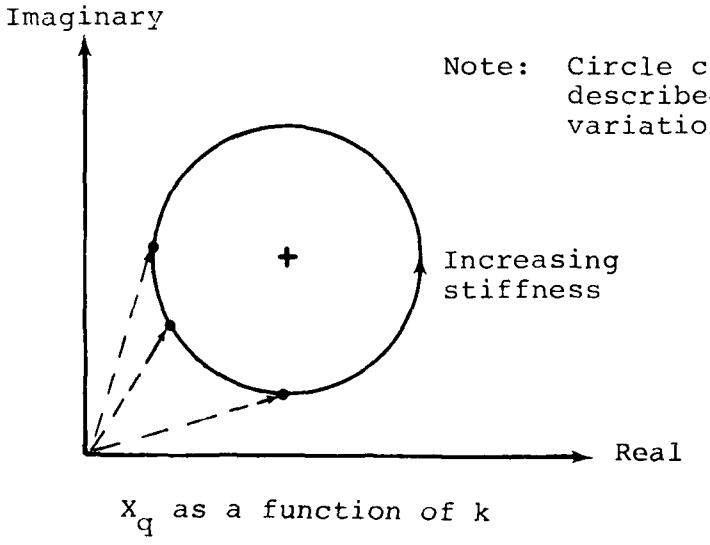

Figure 1. Vincent circle phenomenon.

The nonzero elements in the forcing vector F are F_r, F_s, and F_p. The response equations of interest are

$$x_q = G_{qp} F_p + G_{qr} F_r + G_{qs} F_s \tag{4}$$

$$x_r = G_{rp} F_p + G_{rr} F_r + G_{rs} F_s \tag{5}$$

$$x_s = G_{sp} F_p + G_{sr} F_r + G_{ss} F_s \tag{6}$$

where

G_{qp} is the complex receptance providing the displacement at point q due to a force at point p, etc.

Expressing F_r and F_s in terms of x_r and x_s from Equation (3), and subsequent elimination of x_r and x_s from Equations (4), (5), and (6), gives

$$\frac{x_q}{F_p} = G_{qp} + \frac{k\,(G_{sp} - G_{rp})\,(G_{qr} - G_{qs})}{1 + k(G_{rr} + G_{ss} - G_{rs} - G_{sr})} \tag{7}$$

This may now be rewritten in more general terms as

$$\xi + i\eta = (e + if) + \frac{k(a + ib)}{1 + k(c + id)} \tag{8}$$

where

$$\frac{x_q}{F_p} = \xi + i\eta \tag{9}$$

and a, b, c, d, e, and f are all real. The imaginary part of Equation (8) can be rearranged to the equation of a circle, being

$$\left[\xi - \left(e + \frac{b}{2d}\right)\right]^2 + \left[\eta - \left(f - \frac{a}{2d}\right)\right]^2 = \frac{a^2 + b^2}{4d^2} \tag{10}$$

It is important to note here that the radius of the circular response, as well as the complex coordinates of the center of the circle, may be obtained from these original complex

receptance matrix coupling terms of Equation (10). No iterations in k are necessary; in fact, k drops out of the solution when expressed in this form. Furthermore, it is clearly seen that these circular response properties are purely a function of the imaginary terms (i.e., damping).

Several papers have been published (References 2, 3, and 4) to both mathematically and experimentally substantiate this circular response region, and to employ these circular properties as a possible optimization technique for reducing structural vibration. In a more general sense, Balmford[5] describes the Vincent circle as a method for providing a reduction of vibration in a local area by adjustment of airframe modes such that modal cancellation will take place to reduce the response for one frequency and one loading condition.

STRAIN ENERGY METHOD

Strain energy is an expression for the potential energy of a structural element and is most commonly expressed in matrix form for the static condition as

$$SE = 1/2\ (\delta^T K_e\ \delta) \qquad (11)$$

For the dynamic condition, structural elements possessing the highest strain energies in a given mode of vibration have been shown to be the best candidates for modification to reduce overall structural dynamic amplification.[6] Two approaches are generally considered, as described in the following sections.

Modal Strain Energy Approach

This approach seeks to reduce vibration by detuning a structure natural frequency to a better position with respect to the forcing frequency. Modal strain energy is calculated for each structural element using the mode shape (eigenvector) for the natural frequency to be modified

$$SE = 1/2\ (\phi^T K_e\ \phi) \qquad (12)$$

Elements with the highest strain energies indicate the optimal structural elements to change in order to shift the natural frequency away from the forcing frequency, thereby reducing dynamic amplification.

Forced Response Strain Energy Approach

This is an extension of the modal approach that takes into account the response participation of all modes for a particular load application and excitation frequency, including the effects of structural damping and combined forcing function phase relationships. Therefore, the resultant strain energy of each structural element will be a periodic function in time. Sciarra[6] has done considerable work in this field and has arrived at an expression for the maximum damped forced response element strain energy within the period

$$4(SE)_{max} = \delta_R^T K_e \delta_R + \delta_I^T K_e \delta_I + [(\delta_I^T K_e \delta_I - \delta_R^T K_e \delta_R)^2 + (\delta_R^T K_e \delta_I + \delta_I^T K_e \delta_R)^2]^{1/2} \quad (13)$$

Elements with the highest strain energies indicate the elements that are most responsible for the structural dynamic amplification. Because the forced response strain energy approach gives direct information at the specific excitation frequency of interest, it was selected for comparison to the Vincent circle method.

Figure 2 illustrates an application of the strain energy technique. First, the modal strain energy approach was used to selectively stiffen the structure in order to move a fuselage natural frequency to a higher position above the excitation frequency, thereby reducing the dynamic amplification. A damped forced response analysis of the modified structure was then compared to the original structure, and it was confirmed that an overall vibration reduction had resulted in the fuselage area of interest.

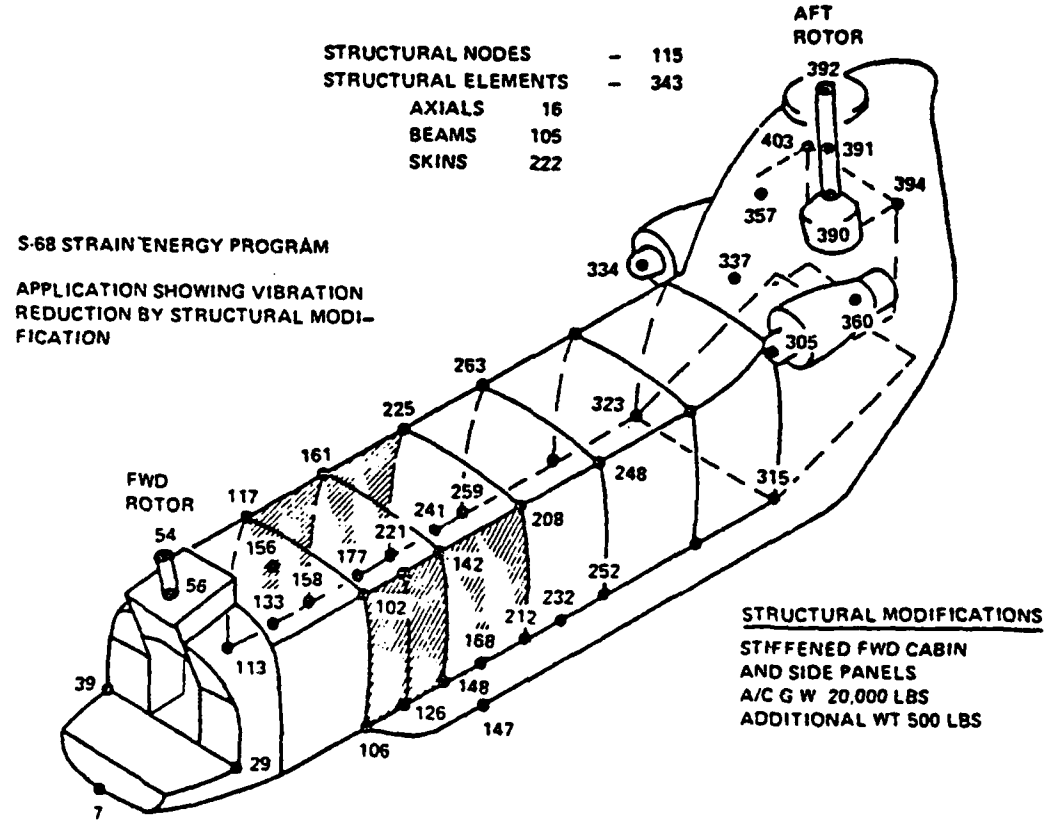

Mode	Original Fuselage Hz	Modified Fuselage Hz	Excitation Frequency 11.45 Hz
7	6.687	6.703	
8	7.879	8.160	
9	8.442	8.494	
10	12.03	12.74 ←	Natural Frequency Changed (Mode No. 10, 4th Elastic Mode) – Mode Amplification Factor Down From 9.1 to 5.0
11	12.52	12.79	
12	14.48	14.82	
13	15.69	16.02	
14	16.95	17.22	
15	18.94	19.06	

A damped forced response analysis comparison of the original and the modified fuselage resulted in a vibration reduction for 99 out of 123 degrees-of-freedom.

Figure 2. Boeing-Vertol CH-47A vibration reduction by structural modification (Reference 6).

PROGRAM OBJECTIVES

The purpose of this contracted study was to evaluate the practical applicability of the Vincent circle method, as compared to the forced response strain energy method, for reducing vibration through realistic structural stiffness optimization. The analytical study was performed on the Model AH-1G helicopter, and the effort was limited to application of a single steady-state main rotor 2/rev (10.8 Hz) vertical excitation force with a goal of minimizing the pilot's seat vertical response.

The Vincent circle method was further investigated for usefulness as applied to evaluating mass changes, damping, and ability to optimize dynamic absorber locations.

ANALYTICAL APPROACH

METHOD OF ANALYSIS

For evaluating the Vincent circle method, the receptance matrix technique previously described offers an attractive and direct means to obtain the response circle radius and center-of-location properties based on a single stiffness (or mass) parameter. However, for a feasibility study of this nature, several important disadvantages also exist in that the receptance matrix technique is not easily adapted for evaluation of the following:

- The sensitivity of the circular response region versus element stiffness (or mass) values.

- A coupled stiffness matrix between two points. In dealing with real structure, rarely are we concerned with a single uncoupled parameter like a simple spring, but rather structural elements behaving more like beams that have coupled stiffness matrices. For example, a single variation in the area moment of inertia (I) of a beam affects both the shear translational and rotational degrees-of-freedom between the two ends of the beam.

- Individual element damping variations while the damping for the remainder of the structure remains uniform.

- Tuning sensitivity of a dynamic absorber at different locations on the structure (i.e., effect of backup structure at absorber location).

Since the purpose of this contracted effort was not to evaluate the merits of the receptance matrix technique, and in order to use the same analytical tool for evaluating both the Vincent circle method and the forced response strain energy method, a straightforward linear NASTRAN[7] analysis was selected for performing the study. Also, due to a unique situation at Bell Helicopter Textron wherein many NASTRAN computer runs can be accomplished quickly and at a low cost, the additional time and cost that would have been required to develop a special purpose receptance matrix manipulation computer program was avoided.

---

[7]THE NASTRAN USER'S MANUAL, NASA SP-222(03) National Aeronautics and Space Administration, Washington, D. C., July 1976.

As applied to the Vincent circle method, this straightforward NASTRAN approach required the evaluation of several iterations in the particular parameter under investigation to develop the circular response region, from which the response circle radius and center-of-location properties were subsequently determined. However, no restrictions were necessary on what parameters could be selected, and more in-depth information was provided as to the characteristics of the circular response region than if the receptance matrix technique had been employed.

The version of NASTRAN used at the time of this study was Level 16.0.5. This particular level of NASTRAN does support strain energy calculations, but only for static analysis. Although desirable, it was found that the NASTRAN internal modifications necessary to incorporate the complex damped forced response strain energy calculations (Equation 13) were beyond the scope of this study. However, by using the Direct Matrix Abstraction Program (DMAP) capability in NASTRAN, the static strain energy module was incorporated into the dynamics frequency response analysis with the following limitations:

- All applied oscillatory loads must be input at zero degrees phase.

- No damping can be included, thus the applied load and response vector have only real components.

These limitations were required because the statics format of the NASTRAN strain energy module is not compatible for processing complex numbers (i.e., only the real part of a complex number is considered). Therefore, the forced response strain energy expression for a structure element responding to a single resultant applied load with zero damping has now been reduced to

$$SE = 1/2\ (\delta_R^T K_e \delta_R) \qquad (14)$$

This results in a strain energy distribution that is a close approximation to the strain energy distribution obtained when a small amount of uniform structural damping is included. For the purposes of this study, this undamped strain energy distribution was acceptable for comparison to the Vincent circle results, wherein a small amount of damping must be included as previously explained.

MATHEMATICAL MODELS

Initial stiffness parameter investigations were conducted using a simple elastic-line NASTRAN model of the AH-1G helicopter (Figures 3 and 4). This elastic-line model was originally developed as an AH-1J (Reference 8) and was later modified into the AH-1G configuration (Reference 9). The structural optimization method showing the most potential for reducing vibration through realistic structural stiffness changes was then applied to minimize pilot's seat vertical response using a large complex built-up NASTRAN model of the AH-1G (Figure 5).[10] The elastic-line model was also used to further evaluate the Vincent circle method as applied to mass, damping, and dynamic absorber parameters.

For use in this study, both the elastic-line and the built-up models of References 9 and 10, respectively, were updated to a basic mission-clean wing configuration. To show the similarity of the two models, a comparison of weight data and natural frequency placements is shown in Table 1. From the natural frequency comparisons, in addition to the obvious absence of landing gear skid modes, it is seen that the elastic-line model has no fuselage torsional modes in the zero to thirty hertz frequency range of interest. This is due to inadequate fuselage torsional mass inertia representation in the elastic-line model which, due to the torsional coupling, is also partially responsible for the differences in pylon roll and fuselage lateral bending modes. Note, however, the close agreement between the two models for the pylon pitch and the first and second fuselage vertical bending modes that are of primary importance in this study. Both the elastic-line and built-up models have the same elastic-line representations for the helicopter tailboom structure.

---

[8] Cronkhite, J. D., and Wilson, W. F., DYNAMIC ANALYSIS OF TWO-PER-REV VIBRATIONS IN THE MODEL AH-1J HELICOPTER - PIP Task No. AH-8-123, Bell Helicopter Textron Report 299-100-021, Fort Worth, Texas, 4 February 1972.

[9] Cronkhite, J. D., XM-97 (20MM) WEAPON ON THE AH-1G - PRELIMINARY DYNAMIC ANALYSIS, Bell Helicopter Textron Interoffice Memo 81:JDC:mb-054, Fort Worth, Texas, 29 May 1973.

[10] Cronkhite, J. D., Berry, V. L., and Brunken, J. E., A NASTRAN VIBRATION MODEL OF THE AH-1G HELICOPTER AIRFRAME, U.S. Army Armament Command Report No. R-TR-64-45, Research Directorate, Gen. Thomas J. Rodman Laboratory, Rock Island Arsenal, Rock Island, Illinois, June 1974.

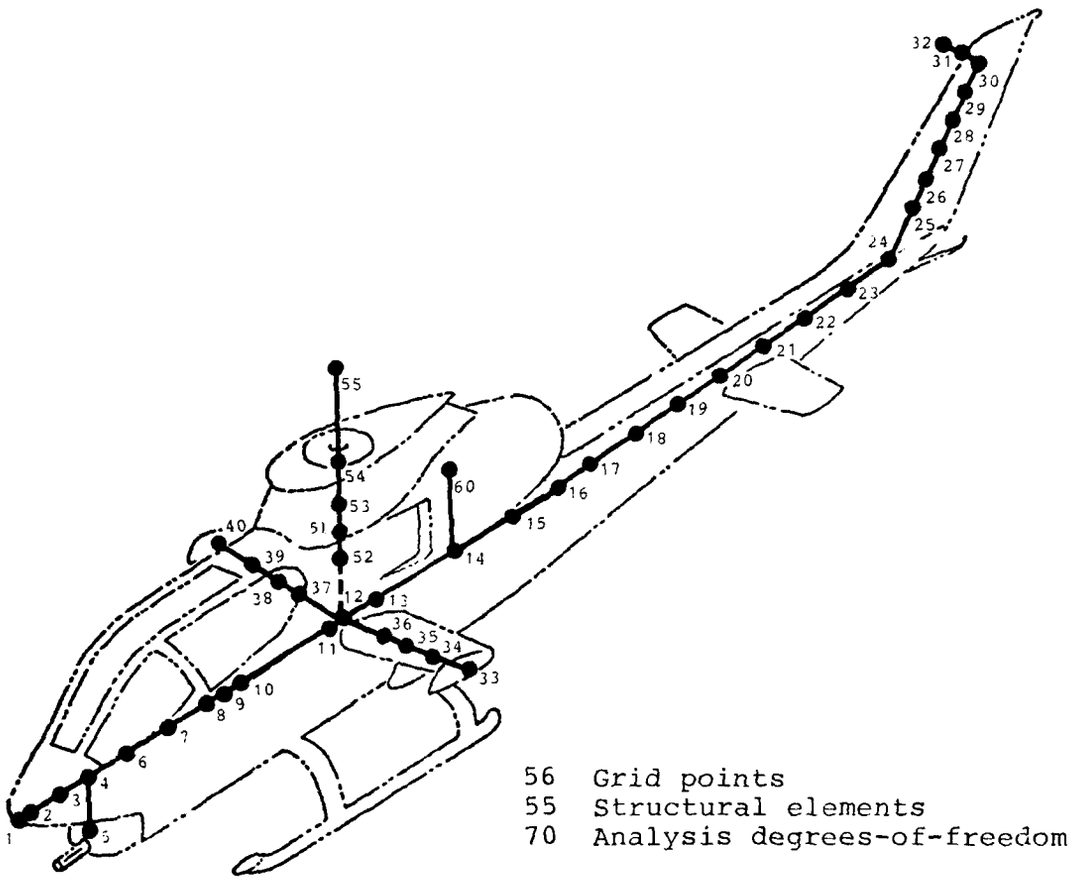

Figure 3. AH-1G elastic-line math model.

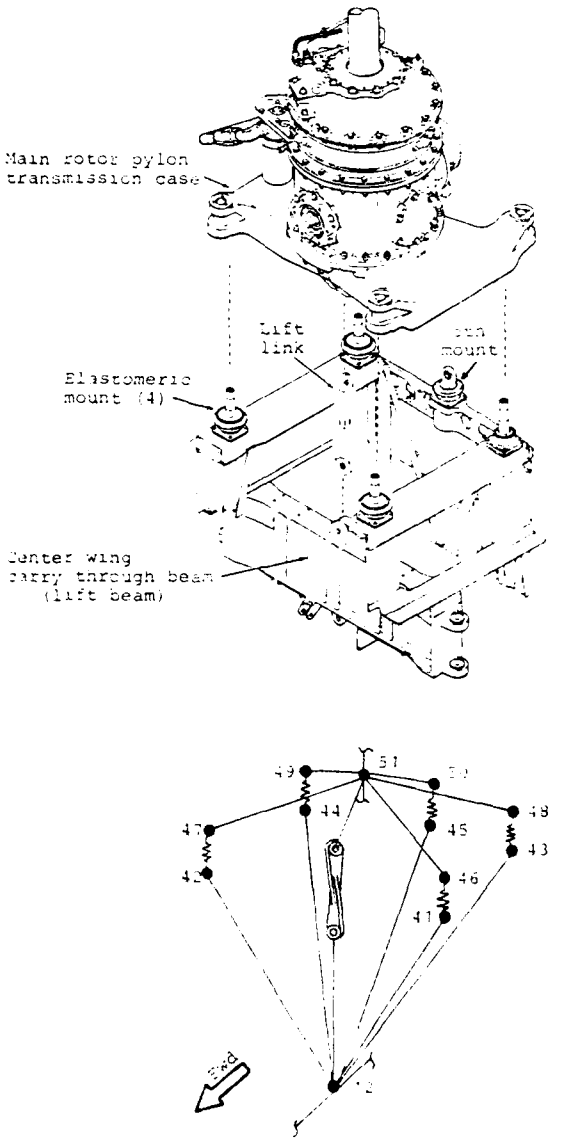

Figure 4. Elastic-line model main rotor pylon.

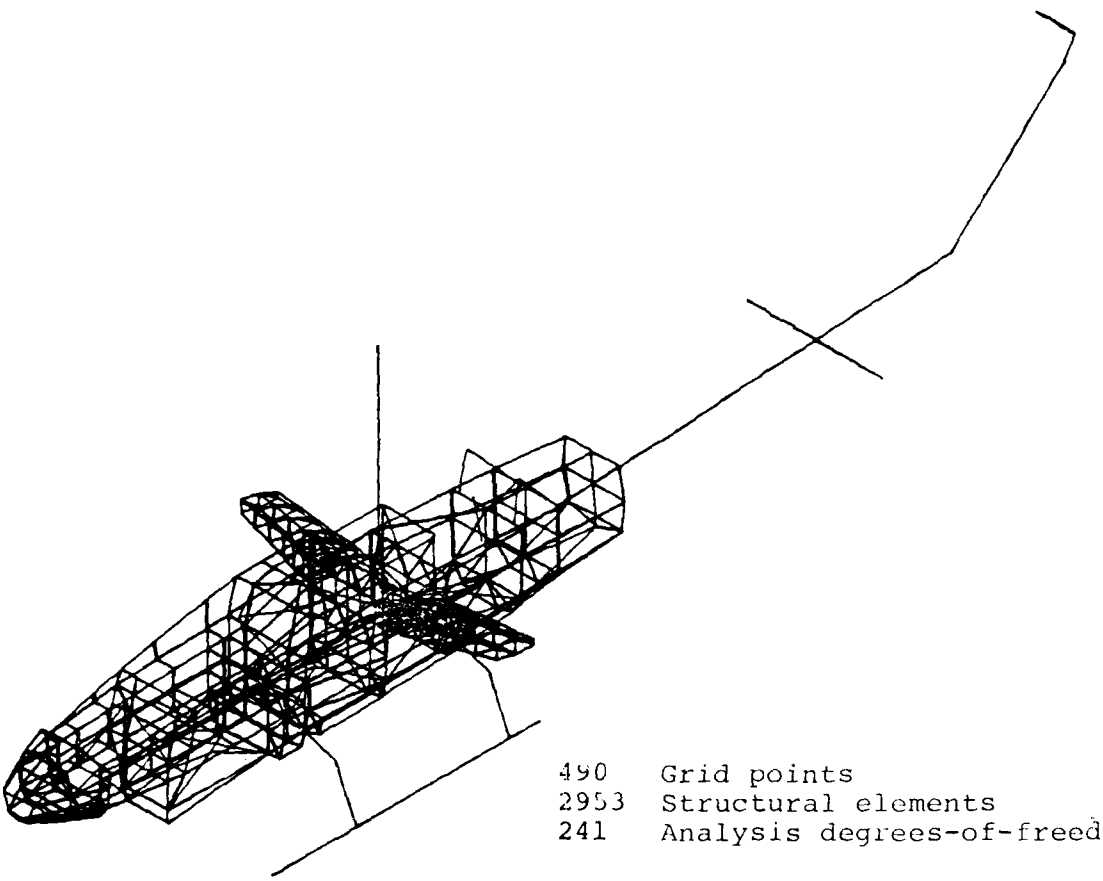

Figure 5. AH-1G built-up math model.

TABLE 1. AH-1G MODEL COMPARISON

Basic Mission-clean Wing	3-D Built-Up Model	Elastic Line Model
Weight Data		
Gross weight (lb)	8394.	8394.
Center-of-gravity Sta (in.)	192.9	193.1
Center-of-gravity BL (in.)	0.0	0.1
Center-of-gravity WL (in.)	70.6	68.7
Inertias Roll ($lb\text{-}in.^2$)	1.139×10^7	1.139×10^7
Inertias Pitch ($lb\text{-}in.^2$)	6.193×10^7	6.200×10^7
Inertias Yaw ($lb\text{-}in.^2$)	5.196×10^7	5.215×10^7
Natural Frequency Data		
Mode Description	(Hz)	(Hz)
M/R pylon pitch	3.03	3.02
M/R pylon roll	3.90	4.24
1st Fuselage lateral bending	7.14	6.80
1st Fuselage vertical bending	7.94	7.93
1st Skid mode	14.57	-
1st Fuselage torsion	15.66	-
2nd Fuselage lateral bending	17.49	16.70
2nd Fuselage vertical bending	17.49	17.86
2nd Skid mode	18.76	-
3rd Skid mode	19.84	-
2nd Fuselage torsion	21.49	-
4th Skid mode	23.43	-
M/R mast lateral bending	25.28	24.79
M/R mast F/A bending	24.97	25.80
5th Skid mode	25.75	-
3rd Fuselage vertical bending	26.96	29.47
6th Skid mode	29.04	-

The AH-1G elastic-line NASTRAN model (including the DMAP ALTER procedure developed for obtaining undamped forced response element strain energy output) is included as Appendix A.

PRACTICAL CRITERION FOR STRUCTURAL STIFFNESS CHANGES

A practical criterion for stiffness change limitations was developed by considering the classical single degree-of-freedom spring/mass/damper dynamic system that has a resonance dynamic amplification factor of 25 for 2 percent damping. This amplification factor can be reduced to 1.1 by either reducing the stiffness by a factor of 0.5, or by increasing the stiffness by a factor of 10, assuming the mass and damping parameters to remain constant. This 0.5 to 10 stiffness factor range seems to be within the limits of practical considerations even though, realistically speaking, structure designed for strength would not have its stiffness reduced by one-half or increased ten-fold without undergoing a considerable redesign effort (i.e., geometric shape factor, type materials, added weight penalties, etc.)

Based on this practical stiffness change criterion, the forced response strain energy and Vincent circle results were compared to determine which was the most promising method for vibration reduction through realistic structural stiffness optimization.

STIFFNESS PARAMETER INVESTIGATIONS

ELASTIC-LINE MODEL ANALYSIS

The forced response strain energy method was used to determine which structural members had the highest forced response strain energies. Using stiffness parameter variations, these members were then analyzed using the Vincent circle method.

Forced Response Strain Energy Results

Figure 6 is a NASTRAN-generated plot showing a side view of the elastic-line model forced response vertical deformation mode shape. The resultant forced response strain energy distribution is shown in Figure 7. The element identification numbers shown are related to the two-digit GRID numbers at each end of the element, as identified in Figures 3 and 4. The strain energy shown for each element is the total due to the resultant six degrees-of-freedom deflections at each end of the element and the element stiffness matrix as calculated by Equation (14). Since the elastic-line model is essentially symmetric and the applied load at the hub is in the vertical direction, only deflections in the vertical plane are contributing significantly to the strain energy calculation. Note how the strain energy distribution compares to what might be expected from examination of the elastic deformation mode shape of Figure 6.

The elastic-line model NASTRAN forced response strain energy output data are presented in Appendix B.

Vincent Circle Results

As previously shown, this circular response property is based on variations involving single parameters only. However, in this study the Vincent circle method was evaluated with respect to realistic element property changes such as AE axial stiffness and EI bending stiffness parameters, wherever applicable, so that the influence of all stiffness coupling terms would be included.

In all cases, a single 1000-pound 2/rev main rotor vertical excitation force was applied and the vertical response of the pilot's seat was calculated. Unless otherwise stated, all Vincent circle calculations were performed assuming 2-percent uniform structural damping.

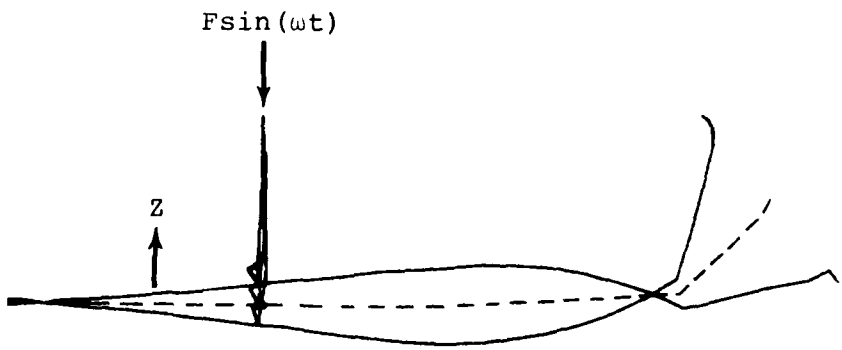

Figure 6. Elastic-line model 2/rev forced response mode shape.

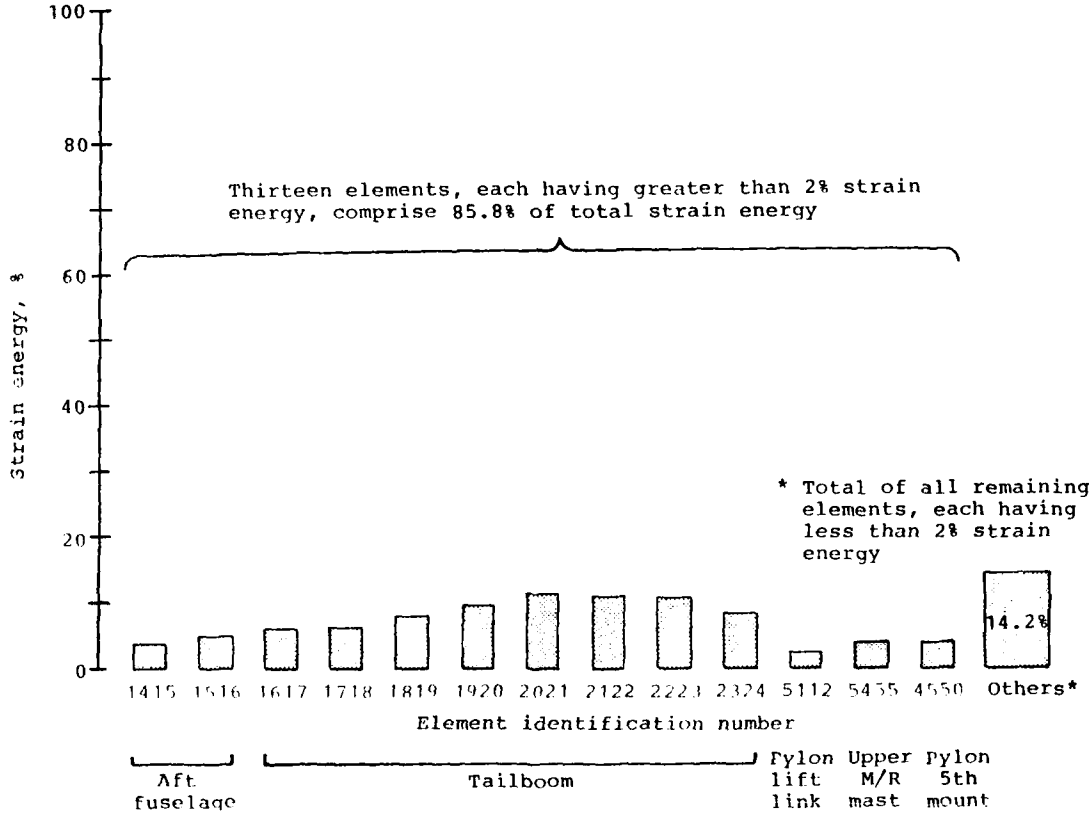

Figure 7. Elastic-line model forced response strain energy distribution.

The first application of this method was to verify the circular response property using the elastic-line model. This was accomplished by evaluation of the AE axial stiffness parameter for the upper main rotor mast segment, as shown in Figure 8. Of particular significance are the zero response at zero stiffness and the sensitivity of response to stiffness variations. The zero response at zero stiffness occurs since the main rotor mast provides the only load path. The baseline stiffness value of the element indicates a low initial amplification factor, and the response is seen to be relatively insensitive to stiffness variations except for drastic changes over a very small range of values where, in reality, the element stiffness is the single parameter responsible for the resonance condition. Since the applied load was directed straight down the mast axis, only the mast AE stiffness parameter was evaluated.

With the circular response property thus verified, the remainder of the thirteen elements showing significant forced response strain energies were evaluated for Vincent circle properties of circle diameter and center location. In each case, all parameters were maintained at their original baseline values except for the particular stiffness parameter under investigation. Aft fuselage and tailboom elements were evaluated separately for both AE and vertical EI stiffness parameter variations. It was found that element AE parameter changes produced a response circle which included the baseline AE stiffness response point, as previously shown for element 5455 in Figure 8. Changes in the element EI parameter were found to produce another response circle, but one that was offset from the baseline EI stiffness response point. Further investigations showed that this offset of the EI response circle was due to the I associated stiffness coupling between beam transverse deflection and beam bending (slope change) degrees-of-freedom. This stiffness coupling offset effect was found to be most pronounced for element 1415 (Figure 9). The pylon lift link, element 5112, and the pylon 5th mount, element 4550, are analogous to axially loaded pin-ended rods so that only AE stiffness parameters were evaluated.

The response circle diameter indicates the maximum response change possible due to a particular element stiffness parameter. A normalized circle diameter distribution is shown in Figure 10. Figure 11 shows the maximum reduction in response due to each element stiffness parameter as determined from its circle diameter and center location. In the case of elements evaluated for both AE and EI stiffness parameters, the parameter providing the maximum reduction in response was selected. Note that the trend of element effectiveness established in Figure 10 is similar to that depicted in Figure 11.

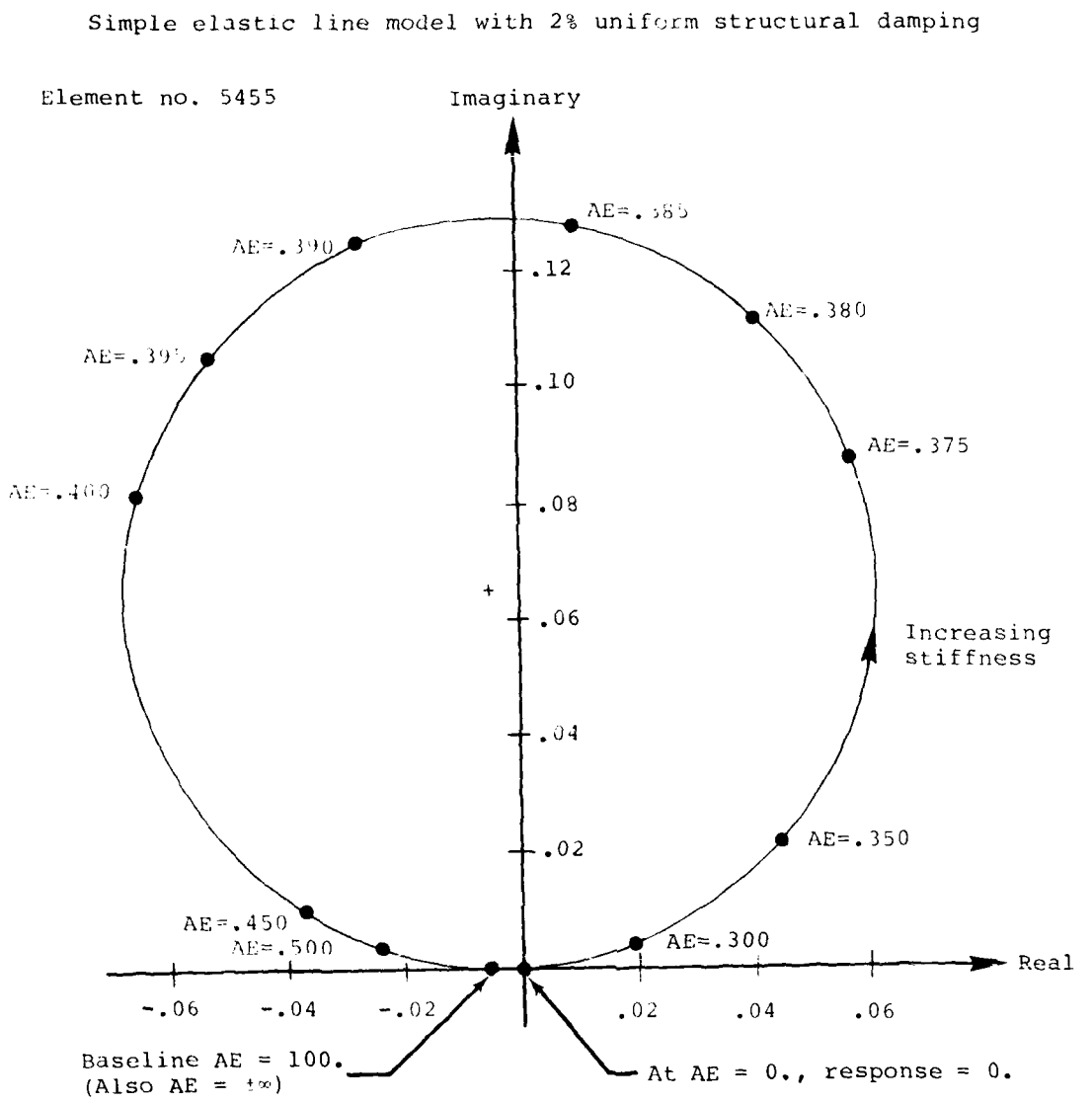

Figure 8. Vincent circle plot for upper main rotor mast segment.

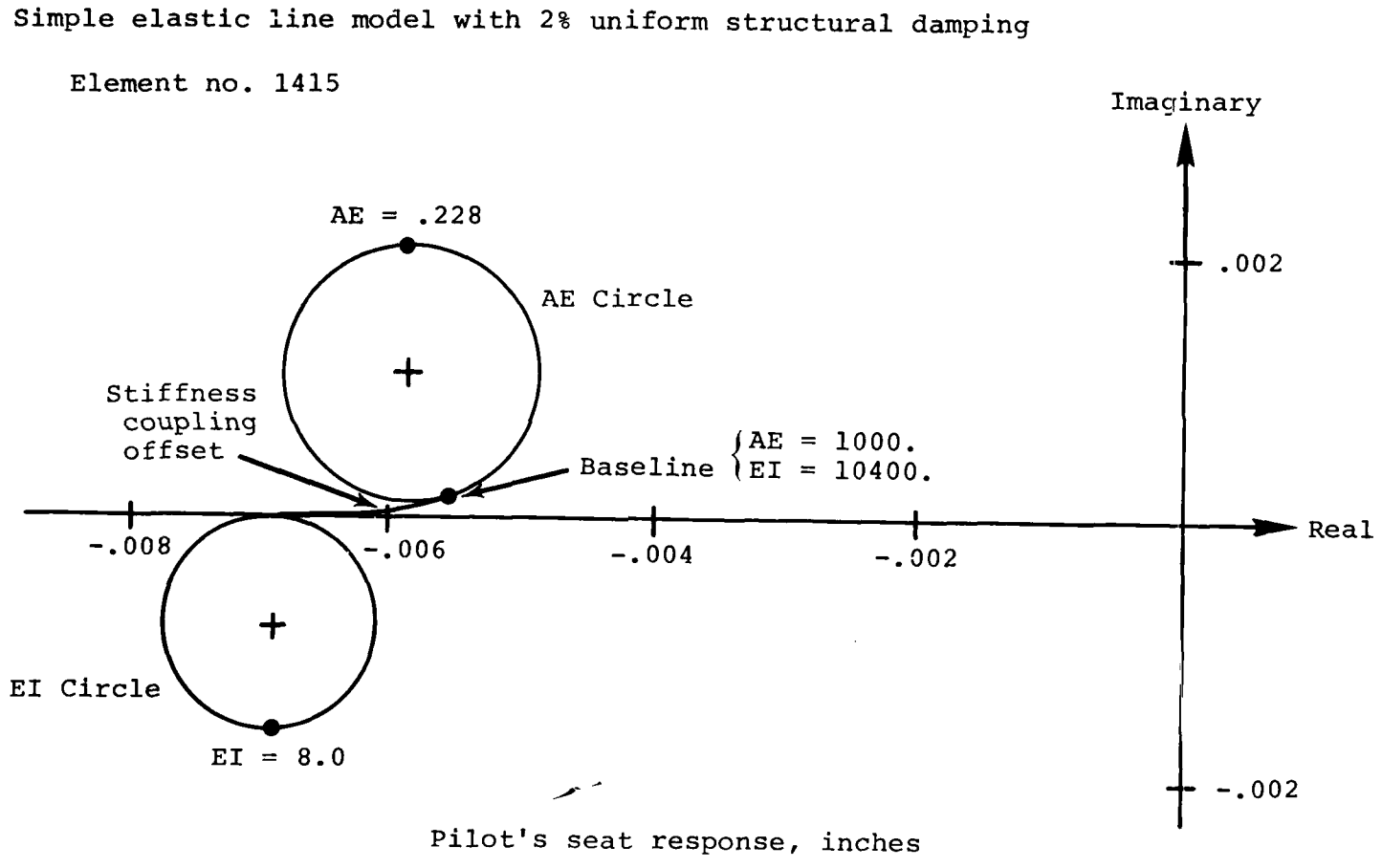

Figure 9. Vincent circle plots for aft fuselage segment.

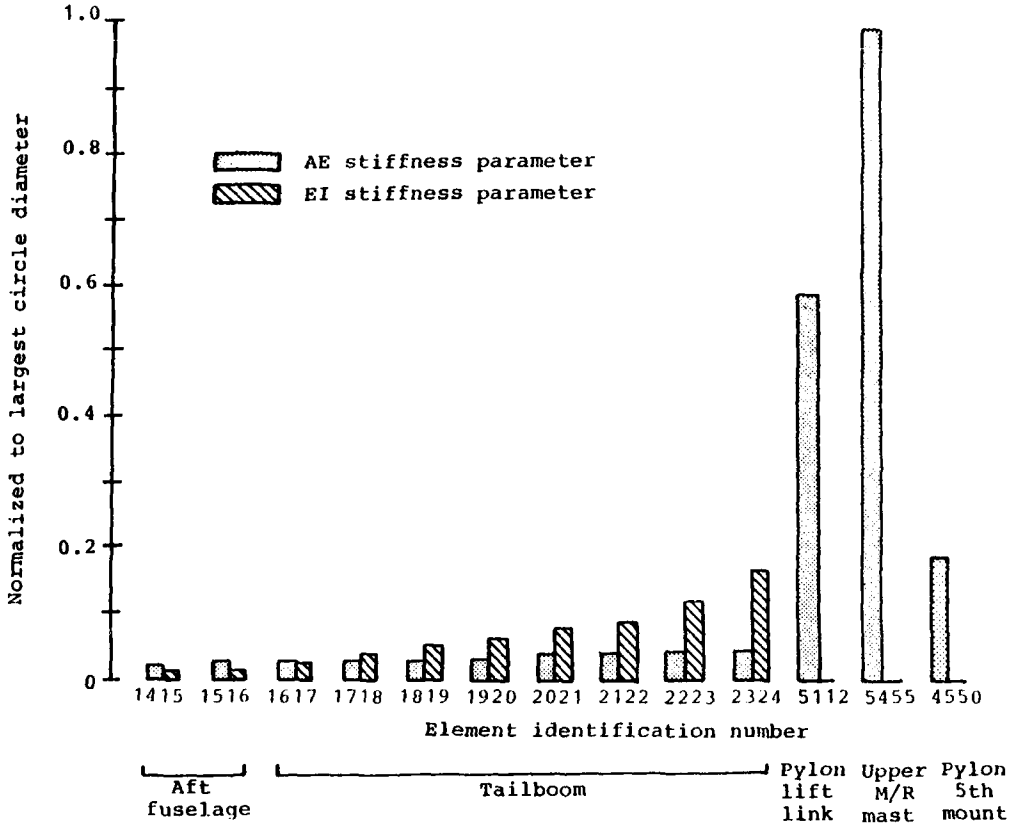

Figure 10. Elastic-line model Vincent circle diameter distribution for pilot's seat response.

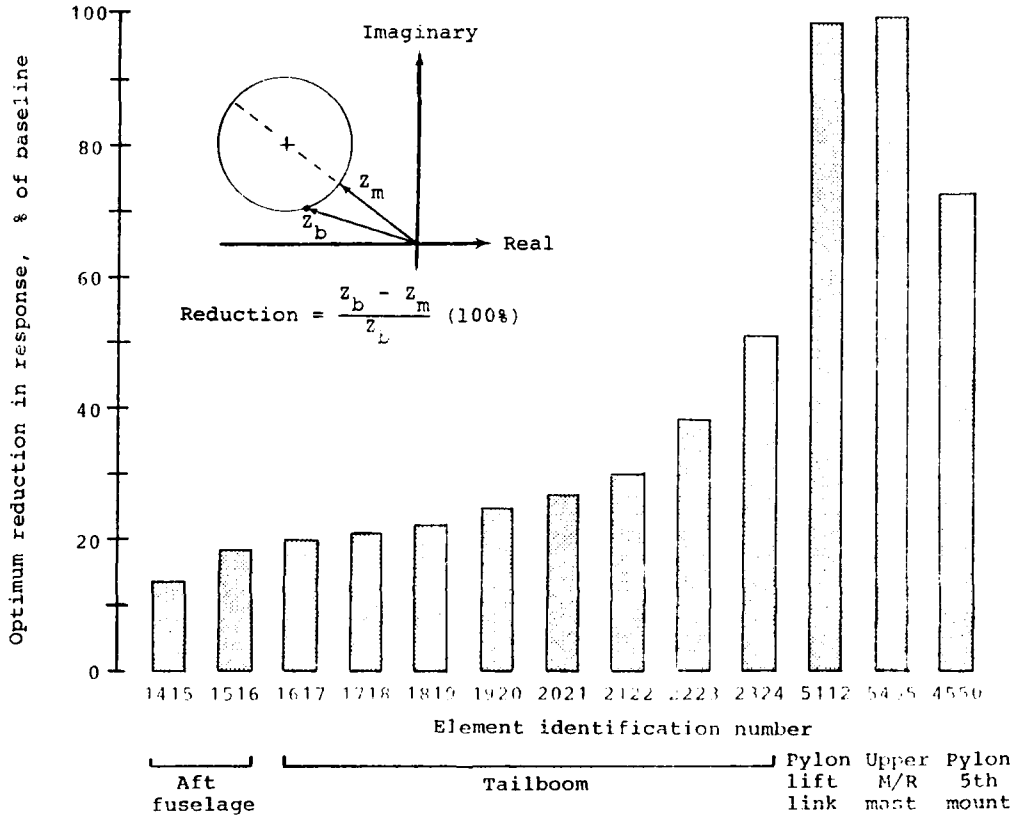

Figure 11. Elastic-line model optimum pilot's seat vibration reduction based on Vincent circle properties.

In other words, in this application the elements with the largest response circle diameters are also capable of achieving the minimum response; however, this is not to be construed as true in all cases.

The most important result to be pointed out is that the Vincent circle properties of circle diameter and center-of-location in the complex plane clearly can be used to determine the minimum response attainable for a particular stiffness parameter; however, no information is provided as to what stiffness value is required to achieve this minimum response. Table 2 shows the drastic and unrealistic stiffness values that were required to produce both the minimum and the maximum pilot's seat vertical response points on the response circle defined by each element stiffness parameter. The two cases where negative stiffnesses are indicated occurred because several elements provided parallel load paths so that a negative stiffness in one element was required to sufficiently reduce the combined elements positive stiffness resultant. In most cases, there is very little difference between the element stiffness values at minimum response and at maximum response (with exceptions for elements 1415, 1516, and 1617 due to their EI response circle offsets (see Figure 9)). Figure 12 further illustrates the stiffness nonlinearity around the response circle by depicting the typical stiffnesses generally found to describe the majority of the circular response region. This inherent property can be somewhat rationalized by considering a single degree-of-freedom model where the dynamic amplification is greatest for the resonance condition and decreases rapidly as the natural frequency is shifted either higher or lower than the excitation frequency.

Strain Energy/Vincent Circle Comparison

Figure 13 compares the undamped forced response strain energy distribution to the 2-percent damped Vincent circle diameter distribution for the same elements of the elastic-line model. Here again, where multiple stiffness parameters were evaluated for the same element, the stiffness parameter producing the largest circle diameter was chosen. It is seen that the Vincent circle method does not give the same distribution picture as the forced response strain energy method. The forced response strain energy method points to the tailboom as the area most responsible for dynamic amplification due to elastic deformation, while the Vincent

TABLE 2. ELASTIC-LINE MODEL ELEMENT STIFFNESS VALUES FOR MINIMUM AND MAXIMUM PILOT'S SEAT RESPONSE

Element No.	Stiffness Parameter Type	% of Baseline Stiffness	
		Minimum Response	Maximum Response
1415	AE	.021%	.024%
	EI	100%	.071%
1516	AE	.011%	.013%
	EI	100%	.027%
1617	AE	.190%	.213%
	EI	100%	.015%
1718	AE	.181%	.206%
	EI	.020%	.021%
1819	AE	.190%	.210%
	EI	.024%	.028%
1920	AE	.168%	.188%
	EI	.027%	.031%
2021	AE	.152%	.168%
	EI	.035%	.041%
2122	AE	.123%	.139%
	EI	.036%	.043%
2223	AE	.115%	.132%
	EI	.056%	.071%
2324	AE	.104%	.118%
	EI	.109%	.190%
5112	AE	-.775%	-.570%
5455	AE	0%	.387%
4550	AE	-167%	-147%

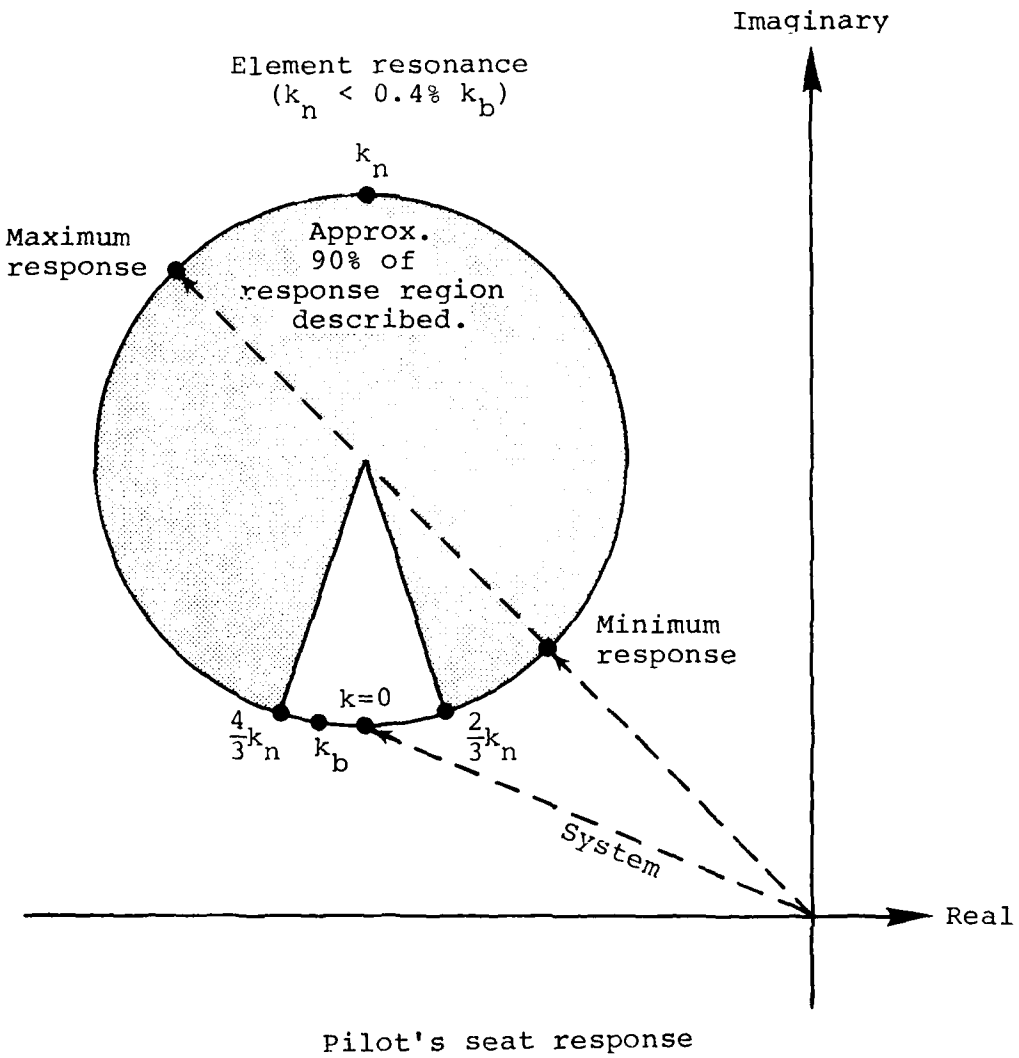

Figure 12. Typical sensitivity of Vincent circle response region.

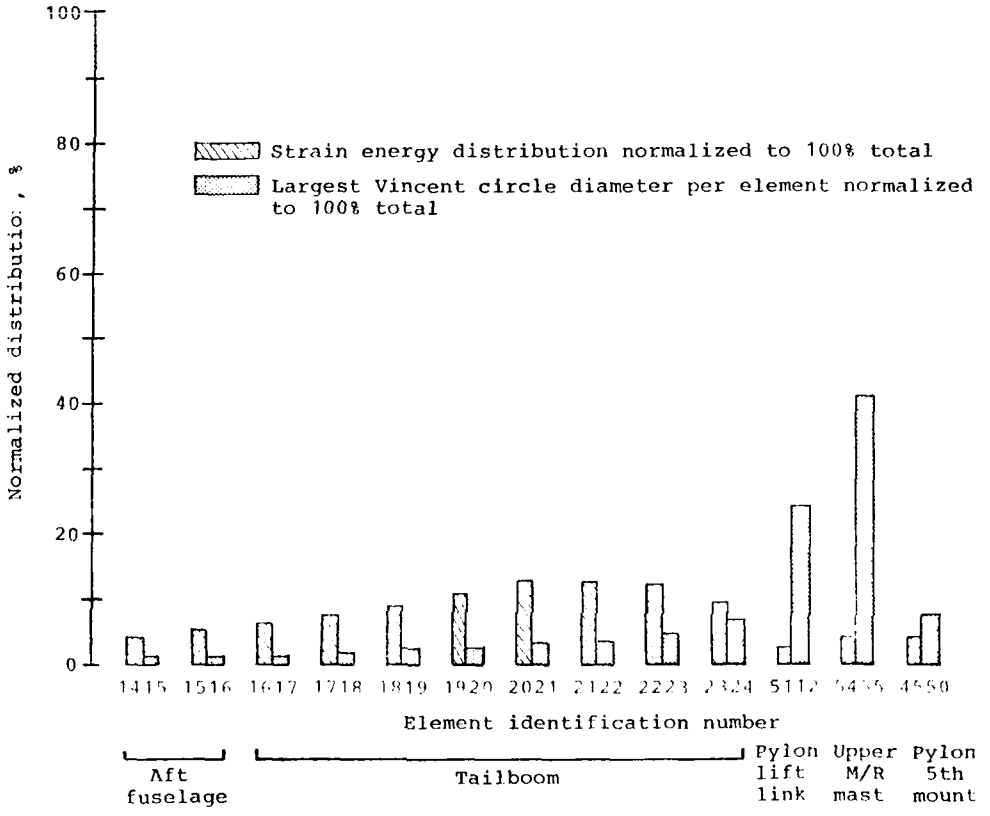

Figure 13. Forced response strain energy comparison to Vincent circle.

circle method points to the pylon as the area having the most potential for reducing vibration at the pilot's seat.

The pylon elements indicated by the Vincent circle method to have the greatest potential for reducing vibration were further evaluated. It was found, as might be strongly suspected from the previous discussion of results, that stiffness variations for these pylon elements within the established confines of the 0.5 to 10 stiffness factor range, even if done collectively, yielded virtually no substantial change in response at the pilot's seat. However, stiffness changes of this same magnitude applied to those tailboom elements initially undergoing substantial elastic deformation, as indicated by the forced response strain energy method, were found to produce significant changes in response at the pilot's seat. Therefore, the forced response strain energy method was determined to be better adapted for vibration reduction through structural stiffness optimization by indicating which structural elements are responsible for the initial dynamic amplification; it was also determined that realistic structural stiffness changes in these elements can efficiently alter the vibration characteristics of the structure.

BUILT-UP MODEL VIBRATION OPTIMIZATION

At this point in the investigations, the selected forced response strain energy method was applied to a large complex built-up NASTRAN model (Figure 5).

A NASTRAN-generated plot of a side view of the built-up model forced response vertical deformation mode shape is shown in Figure 14. The resultant undamped forced response strain energy distribution as compared to the distribution for the elastic-line model is shown in Figure 15. The elastic-line model element identification numbers were retained on the figure for reference. Note the similarity of the two distributions. In the case of the aft fuselage and main rotor mast elements, the single element representation of the elastic-line model has been replaced in the built-up model by more detailed modeling involving many elements more uniformly sharing the load, and each accounts for a smaller percentage of the total strain energy.

Previous analyses[6] have verified that the most dynamically efficient structure for a given mode of vibration is one with a uniform energy distribution. Therefore, the most efficient structural stiffness modifications incorporated for pilot's seat vibration reduction should also result in a more uniform strain energy distribution.

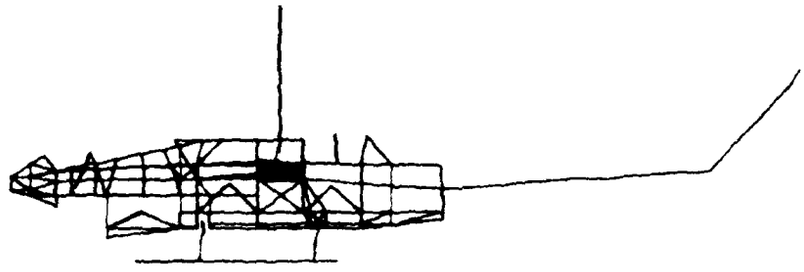

Undeformed shape

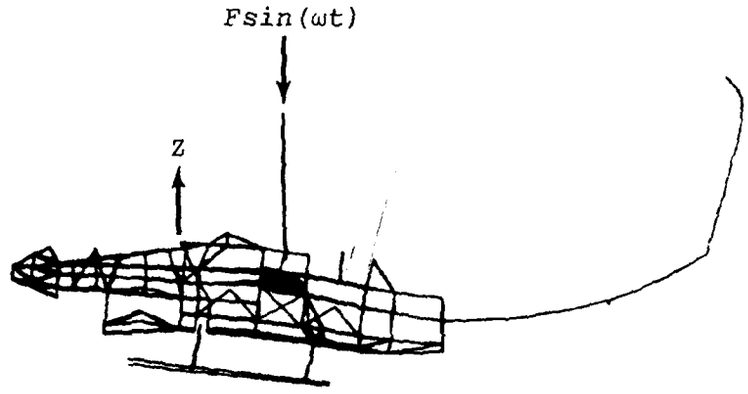

Deformed shape

Figure 14. Built-up model 2/rev forced response mode shape.

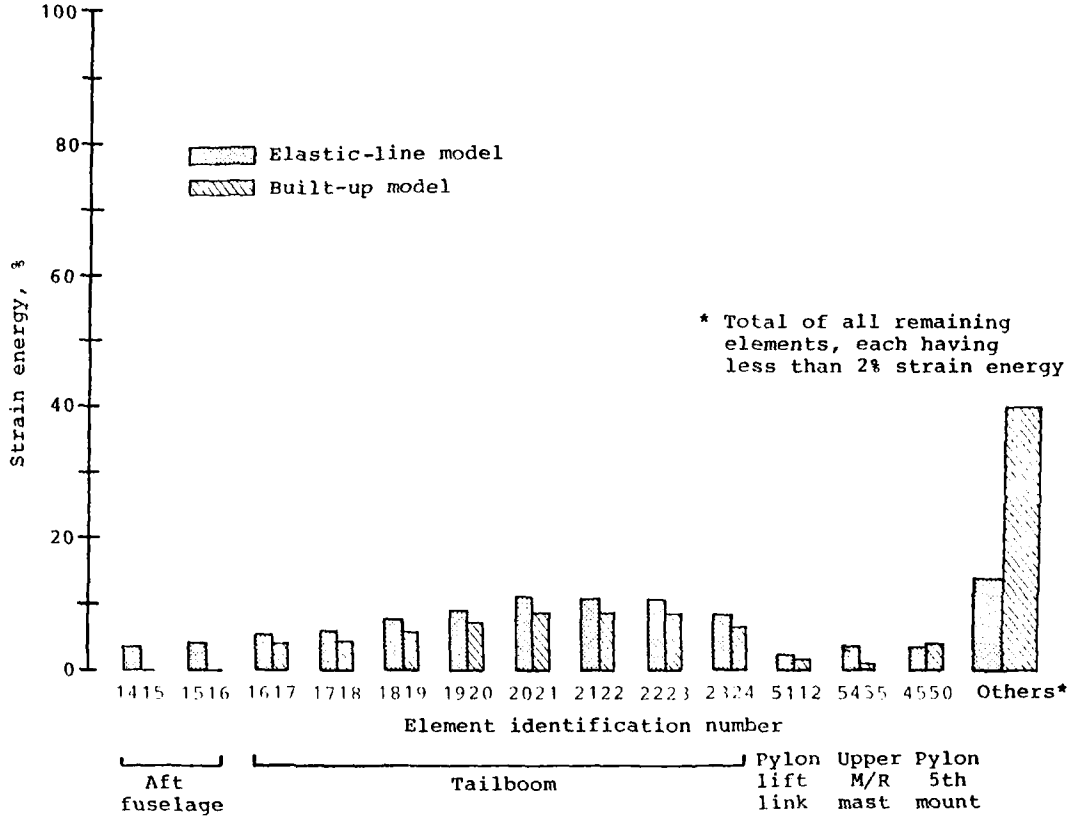

Figure 15. Comparison of forced response strain energy distributions.

From the baseline forced response strain energy distribution, the tailboom elements are seen to possess the most strain energy and were selected as the best candidates for stiffness modifications. The first step was to evaluate both extremes of the selected practical stiffness criterion range. For the stiffer case, the tailboom element with the most strain energy was made ten times stiffer, and the other tailboom elements were made stiffer according to their baseline strain energy ratio. For the softer case, the tailboom element with the least strain energy was made one-half as stiff, and the other tailboom elements were reduced in stiffness according to their baseline strain energy ratio (an additional criterion had to be imposed here - the resultant element stiffness could not be increased because of this strain energy ratio scheme used). The strain energy ratio scheme is shown in further detail in Table 3, along with the accompanying results. In both of these cases the resultant strain energies are more uniformly distributed. In both cases, the pilot's seat response increased in magnitude, but for the stiffer case the response changed phase. This result indicates that a proper stiffness increase, being within the selected practical stiffness criterion range, would result in an absolute zero response at the pilot's seat. Two additional stiffness iterations were required to achieve the desired results. In each case the selected stiffness ratio was applied to tailboom element number 4014220 (largest baseline strain energy) and the other tailboom elements were made stiffer according to their baseline strain energy ratio. As shown in Table 3, it was found that a maximum stiffness increase of 375 percent resulted in near zero response at the pilot's seat and reduced the total strain energy in the tailboom by 46 percent. This also resulted in a slight increase in the strain energies of the two tailboom elements nearest the fuselage. Additional selective stiffening of the tailboom could, no doubt, produce the same zero response results with a more uniform strain energy distribution; however, as it was not the purpose of this study to develop a general optimization procedure, further investigations in this area were not pursued.

A better interpretation of these results may be gained from examination of the simplified forced response mode shapes shown in Figure 16. Here it can easily be seen how the deformed mode shape was altered through the stiffness modifications to place the pilot's seat at a node point.

Although in the foregoing analysis it was possible to achieve zero dynamic response at a particular point under a unique set of circumstances, in no way should these results be interpreted as implying that zero response is always attainable

TABLE 3. BUILT-UP MODEL PILOT'S SEAT VIBRATION REDUCTION

Tailboom Element Identification Number		Baseline		Maximum $(SE)_j$ Made 10X Stiffer		Minimum $(SE)_j$ Made 0.5X Stiffer		Optimized For Minimum Response	
Elastic Line Model (Ref)	3-D Built-Up Model	Unitized Stiffness Ratio	Strain Energy $(SE)_j$ (%)	Stiffness Ratio Applied S_j	Resulting Strain Energy (%)	Stiffness Ratio Applied S_j	Resulting Strain Energy (%)	Stiffness Ratio Applied S_j	Resulting Strain Energy (%)
(1617)	3003170	1.0	4.06	4.72	2.59	0.63	3.69	2.24	5.50
(1718)	3173380	1.0	4.50	5.23	2.11	0.70	4.00	2.49	4.61
(1819)	3383590	1.0	5.72	6.65	1.71	0.89	4.31	3.16	3.84
(1920)	3593800	1.0	7.10	8.26	1.41	1.0	5.03	3.92	3.27
(2021)	3804010	1.0	8.49	9.87	1.20	1.0	6.31	4.69	2.85
(2122)	4014220	1.0	8.60	10.0	1.02	1.0	6.68	4.75	2.50
(2223)	4224430	1.0	8.36	9.72	0.91	1.0	6.75	4.62	2.28
(2324)	4434520	1.0	3.23	3.76	0.80	0.50	5.36	1.78	2.04
	4524640	1.0	3.31	3.85	0.72	0.51	5.48	1.83	1.88
	Totals =		53.37		12.47		47.61		28.77
1st Fus. vert. mode		7.94 hz		10.58 hz		7.49 hz		9.94 hz	
Pilot's seat response		-.005508 in		.022153 in		-.005874 in		-.000003 in	

$$S_j = \frac{(SE)_j}{8.60} (10.) \qquad S_j = \frac{(SE)_j}{3.23} (0.5) \qquad S_j = \frac{(SE)_j}{8.60} (4.75)$$

$$\{S_j \geq 1.0\}$$

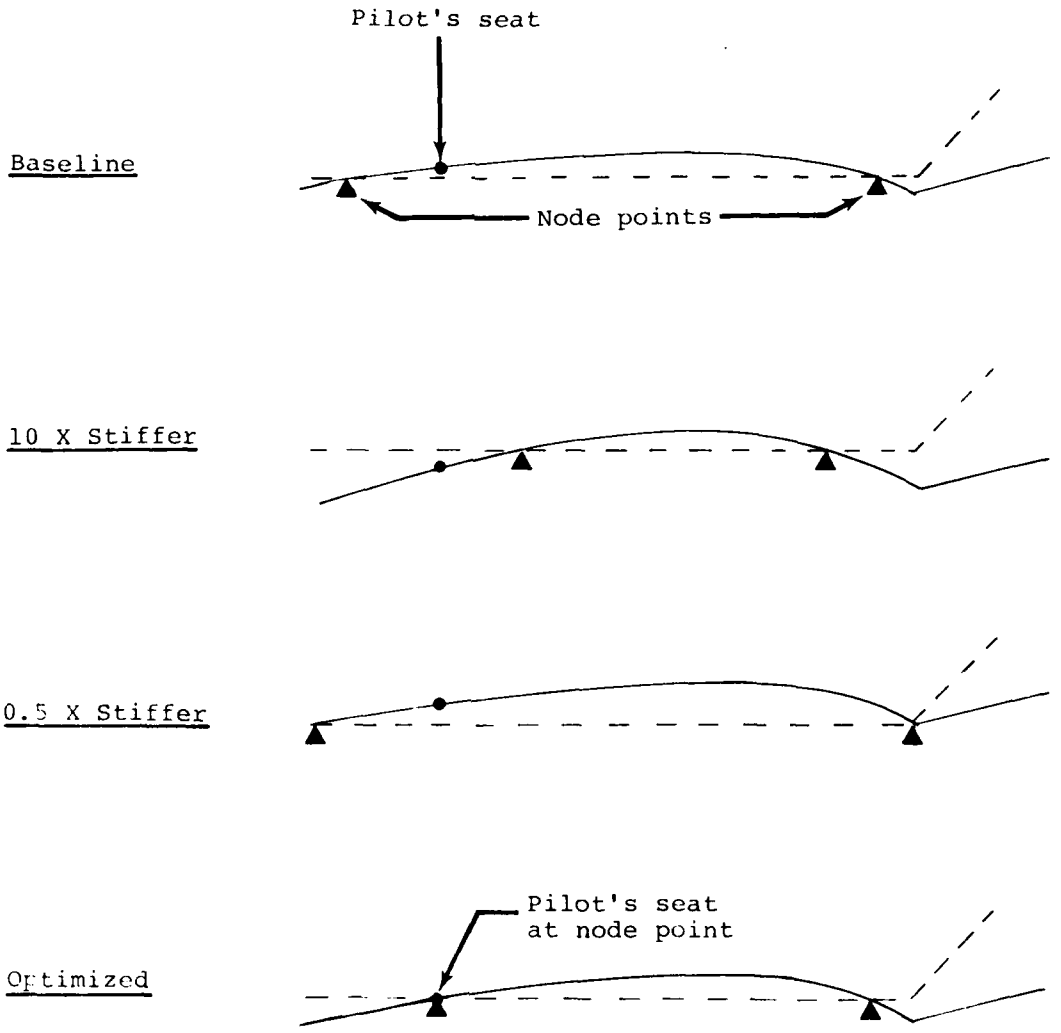

Figure 16. Simplified built-up model forced response mode shapes showing vibration optimization process.

through any type of structural modification. As previously explained in the introduction, many factors need to be considered. Also, for the purposes of this study, no change in mass was considered for any of the stiffness changes evaluated. One of the next most logical steps necessary for any realistic vibration optimization program would be to evaluate the combined effects of both stiffness and the associated weight change. The end product is, of course, a minimum vibration environment obtained through optimization of a structure within a given set of practical criteria.

FURTHER EVALUATION OF THE VINCENT CIRCLE

The Vincent circle phenomenon was further evaluated for mass tuning, damping, and dynamic absorber parameters using the elastic-line model and a simple add-on single degree-of-freedom spring-mass-damper system.

MASS PARAMETER RESULTS

Element mass parameter changes were found to describe the same circle that stiffness changes produce, only the increasing mass traced out the circle in the opposite direction. Data points on the example shown in Figure 17 have been somewhat exaggerated for clarity.

DAMPING PARAMETER RESULTS

Damping is usually not considered as a practical method of effectively altering airframe structural vibration. As shown in Figure 18, both the maximum amplification and the potential of the element for vibration control are greatly reduced by small increases in element damping.

DYNAMIC ABSORBER PARAMETER RESULTS

The adopted procedure for investigating dynamic absorber parameters was to evaluate the effectiveness of one absorber for attenuating 2/rev vertical vibration at the pilot's seat when placed at different locations on the structure; and then, to compare these results to the maximum reductions in pilot's seat response obtained from element stiffness Vincent circle properties at these same locations (as described in Figure 11). The adopted approach does not imply that any such relation between Vincent circle predictions and optimum dynamic absorber locations exists, or has been reported to exist.

The dynamic absorber energy absorption potential was kept constant by maintaining a 25-pound absorber mass and a 0.2% absorber damping coefficient. This required several absorber spring stiffness iterations to achieve the proper tuning of the dynamic absorber at each location due to the different boundary conditions (i.e., backup structure stiffness) which exists throughout the structure. In each case the dynamic absorber was positioned in the vertical direction for reducing pilot's seat vertical vibration. For this study seven dynamic absorber locations were evaluated and the results are shown in Figure 19 as compared to the maximum response reduction distribution obtained from the element stiffness Vincent circle properties.

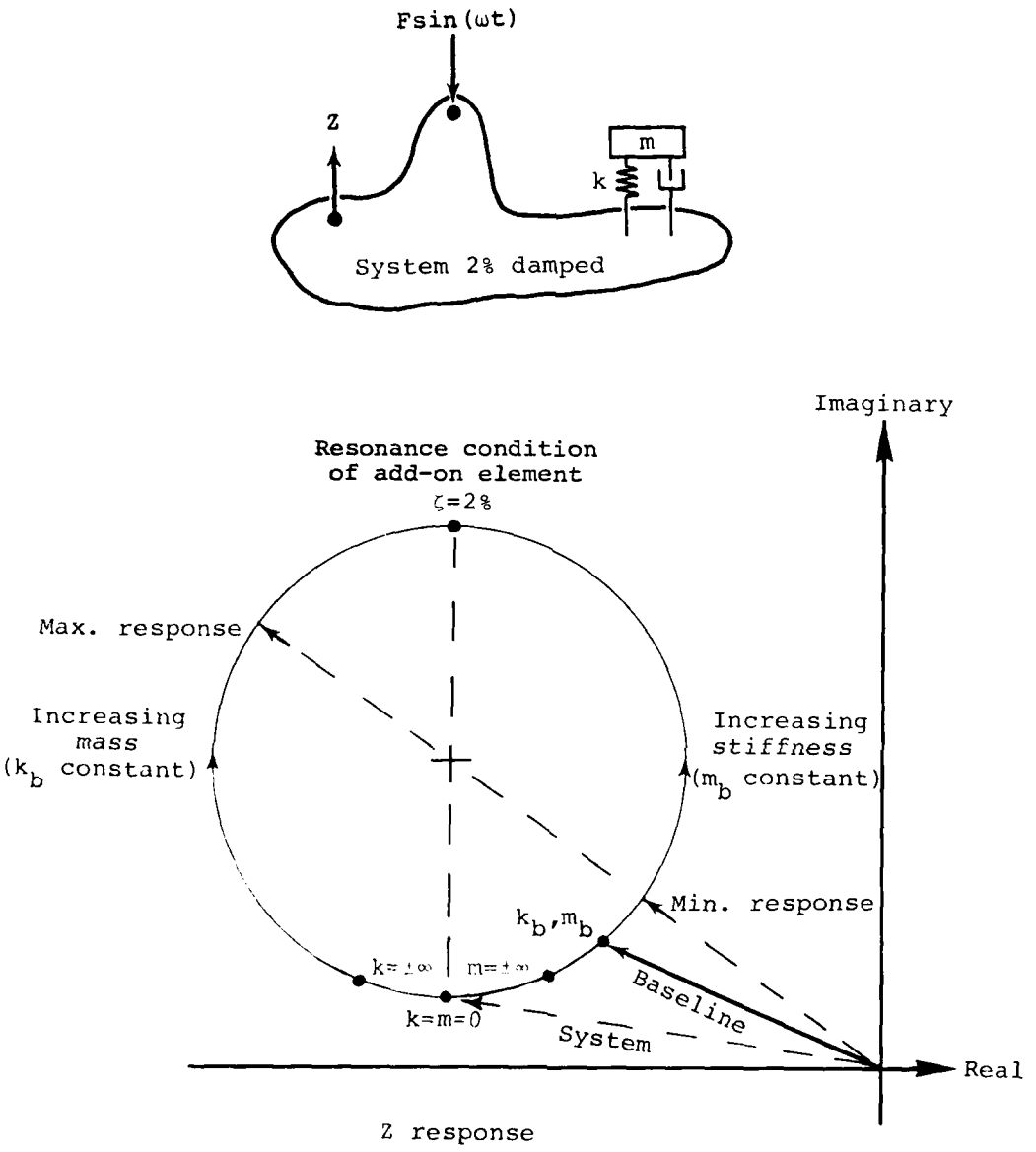

Figure 17. Typical Vincent circle stiffness/mass response region relationships.

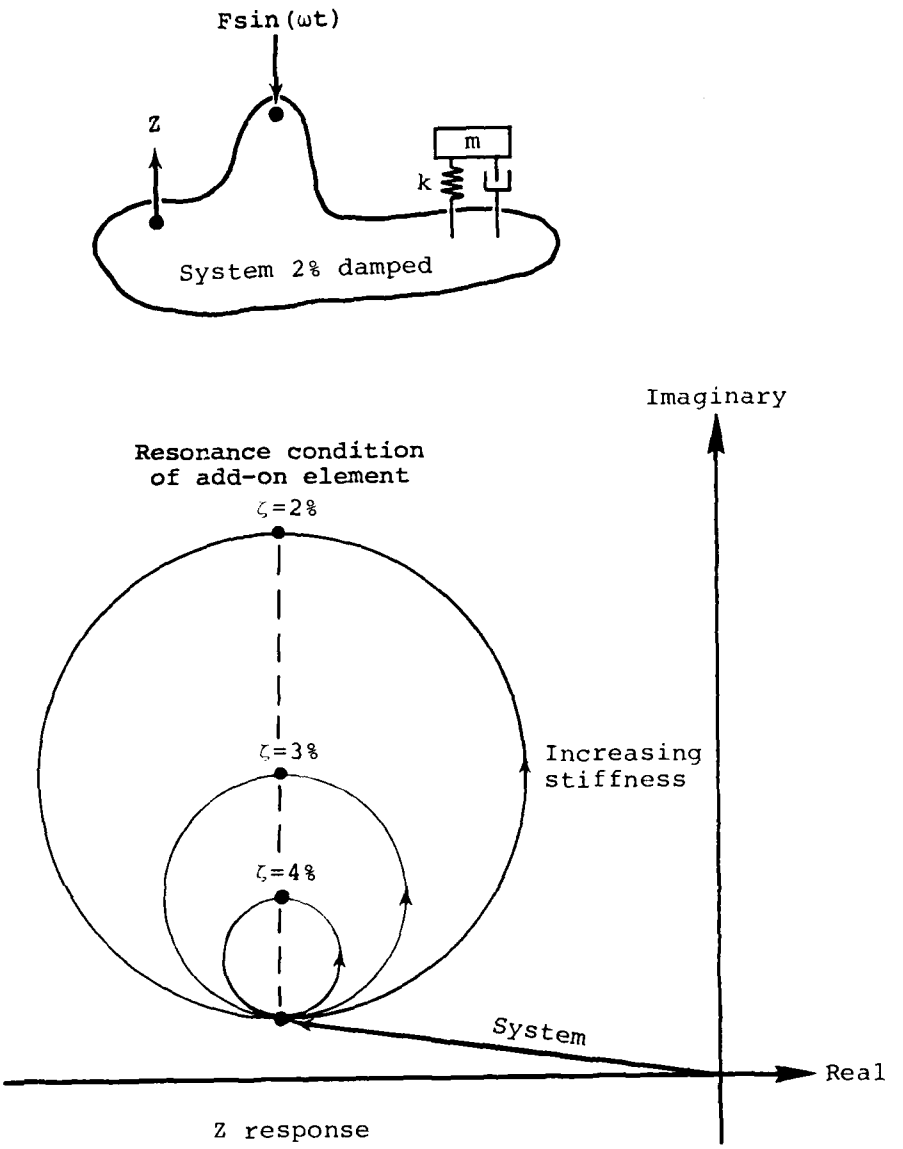

Figure 18. Effect of damping on typical Vincent circle response region.

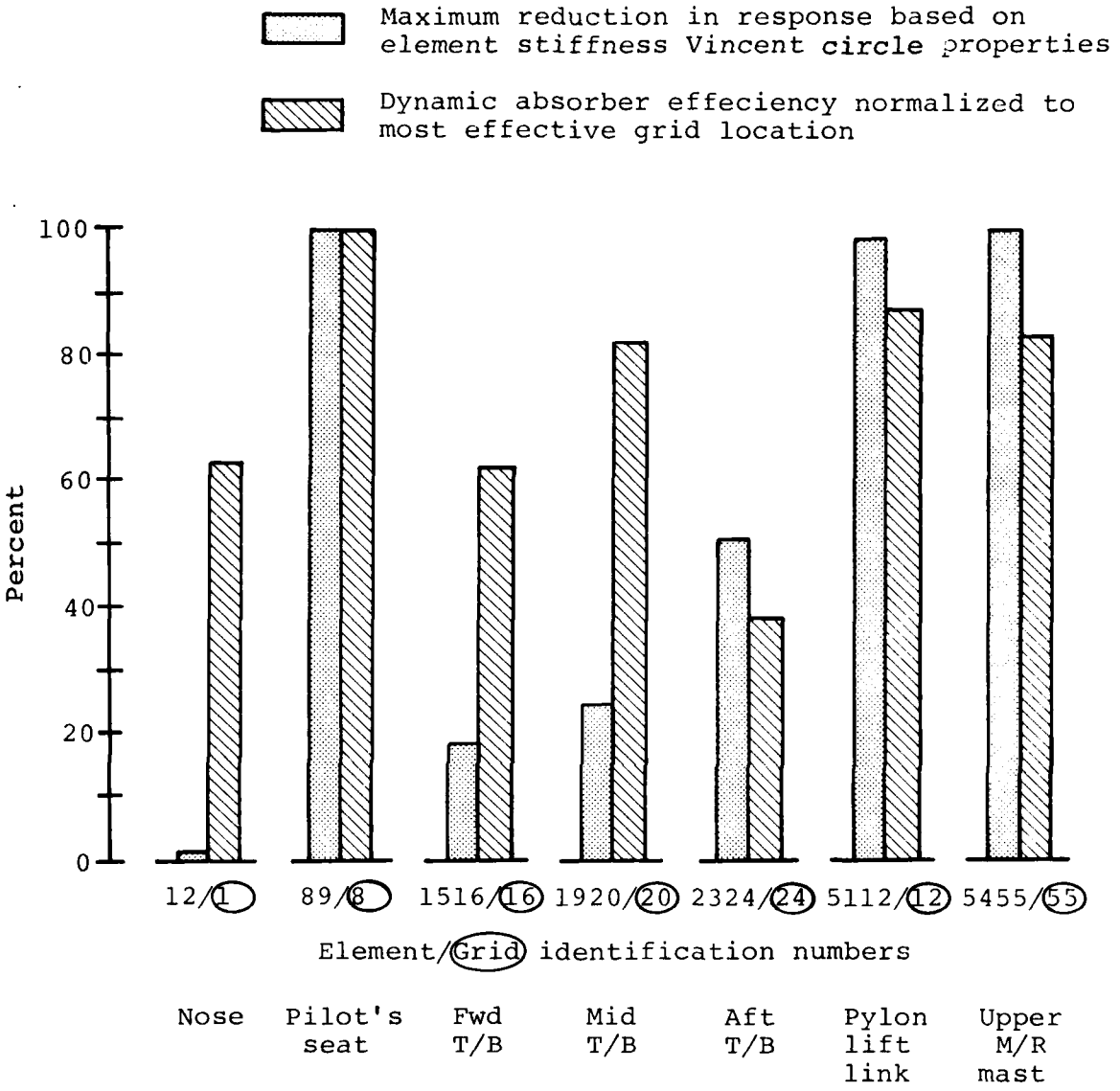

Figure 19. Comparison of Vincent circle properties to dynamic absorber location effectiveness for reducing pilot's seat vibration.

Examination of the dynamic absorber location effectiveness shows that the most efficient location for reducing pilot's seat vibration is at the pilot's seat; but, it also shows that a remote absorber located either at the top of the main rotor mast (grid 55), at the pylon lift link (grid 12), or at the middle of the tailboom (grid 20), would also be significantly effective for reducing vibration at the pilot's seat.

Use of the Vincent circle properties shows that both elements 89 and 5455 are capable of reducing the pilot's seat vibration by 100%. However, these results are inconclusive because any element providing the only load path is ultimately capable of reducing the pilot's seat response to zero if its stiffness is reduced to zero. Further examination of the comparisons shown in Figure 19 shows no definite trends to indicate that the Vincent circle method can be applied to predict optimum dynamic absorber locations.

CONCLUSIONS

The Vincent circle property of a circular response region has been examined and verified by straightforward linear analysis. This property would certainly be of value to the dynamicist for evaluation of a localized portion of structure known to be in, or very near, resonance and which could be controlled by changes involving only a few parameters.

However, for vibration reduction through optimization of an airframe structure where many elements are involved, the forced response strain energy method was found to be more suitable than the Vincent circle method by indicating which structural elements are most responsible for the elastic dynamic amplification. Practical parameter modifications of these elements will most significantly alter the airframe structural dynamic characteristics to reduce vibration. For the more detailed analysis involving complex applied loads, phasing, and damping, the damped forced response strain energy method has the potential benefit of rapid evaluation and optimization of structural vibratory response, which would be particularly beneficial in the predesign stages of an aircraft.

REFERENCES

1. Vincent, A. H., A NOTE ON THE PROPERTIES OF THE VARIATION OF STRUCTURAL RESPONSE WITH RESPECT TO A SINGLE STRUCTURAL PARAMETER WHEN PLOTTED IN THE COMPLEX PLANE, Westland Helicopters Limited Report GEN/DYN/RES/010R, Yeovil, Somerset, England, September 1973.

2. Done, G. T. S., and Hughes, A. D., THE RESPONSE OF A VIBRATING STRUCTURE AS A FUNCTION OF STRUCTURAL PARAMETERS, Journal of Sound and Vibration, Vol. 38, No. 2, 1975, pp. 255-266.

3. Done, G. T. S., and Hughes, A. D., REDUCING VIBRATION BY STRUCTURAL MODIFICATION, Vertica, Vol. 1, No. 1, 1976, pp. 31-38, (paper presented at the First European Rotorcraft and Powered Lift Aircraft Forum at Southampton, September 22-24, 1975).

4. Done, G. T. S., Hughes, A. D., and Webby, J., THE RESPONSE OF A VIBRATING STRUCTURE AS A FUNCTION OF STRUCTURAL PARAMETERS - APPLICATION AND EXPERIMENT, Journal of Sound and Vibration, Vol. 49, No. 2, 1976, pp. 149-159.

5. Balmford, D. E. H., THE CONTROL OF VIBRATION IN HELICOPTERS, Aeronautical Journal, Vol. 81, No. 794, February 1977, pp. 63-67.

6. Sciarra, J. J., USE OF THE FINITE ELEMENT DAMPED FORCED RESPONSE STRAIN ENERGY DISTRIBUTION FOR VIBRATION REDUCTION, Boeing-Vertol Company Report D210-10819-1, U.S. Army Research Office - Durham, Durham, North Carolina, July 1974.

7. THE NASTRAN USER'S MANUAL, NASA SP-222(03) National Aeronautics and Space Administration, Washington, D. C. July 1976.

8. Cronkhite, J. D., and Wilson, W. F., DYNAMIC ANALYSIS OF TWO-PER-REV VIBRATIONS IN THE MODEL AH-1J HELICOPTER - PIP Task No. AH-8-123, Bell Helicopter Textron Report 299-100-021, Fort Worth, Texas, 4 February 1972.

9. Cronkhite, J. D., XM-97 (20MM) WEAPON ON THE AH-1G - PRELIMINARY DYNAMIC ANALYSIS, Bell Helicopter Textron Inter-office Memo 81:JDC:mb-054, Fort Worth, Texas, 29 May 1973.

10. Cronkhite, J. D., Berry, V. L., and Brunken, J. E., A NASTRAN VIBRATION MODEL OF THE AH-1G HELICOPTER AIRFRAME, U. S. Army Armament Command Report No. R-TR-64-45, Research Directorate, Gen. Thomas J. Rodman Laboratory, Rock Island Arsenal, Rock Island, Illinois, June 1974.

APPENDIX A

AH-1G ELASTIC-LINE NASTRAN MODEL


```
ID HANSON,HHT
APP DISP
SOL 8,0
TIME 10
DIAG 8,14,19
$$$$$$$$$$$$$$$$$$$$$$$$$$$$$$$$$$$$$$$$$$$$$$$$$$$$$$$$$$$$$$$$$$$$$$$$
$$$$$$$$$$$$$$$$$$$$$$$$$$$$$$$$$$$$$$$$$$$$$$$$$$$$$$$$$$$$$$$$$$$$$$$$
$                                                                      $
$    NASTRAN LEVEL 16.0.5  /  RIGID FORMAT SOLUTION 8  /  SERIES N     $
$                                                                      $
$   ALTER PACKAGE FOR UNDAMPED FORCED RESPONSE ELEMENT STRAIN ENERGY   $
$                                                                      $
$  NASTRAN LEVEL 16.0.5 DOES NOT SUPPORT ELEMENT STRAIN ENERGY         $
$  CALCULATIONS FOR ANY SOLUTION OTHER THAN RIGID FORMAT SOLUTION 1    $
$  (STATICS).  THIS ALTER PARTITIONS THE OUTPUT FREQUENCY RESPONSE     $
$  DATA BLOCKS TO SIMULATE A STATICS SOLUTION BEFORE PASSING THEM      $
$  TO THE STRAIN ENERGY CALCULATION MODULE (GPFDR).                    $
$                                                                      $
$  RESTRICTIONS ARE:                                                   $
$     1.  ALL APPLIED LOADS MUST BE APPLIED AT ZERO DEGREES PHASE      $
$     2.  NO DAMPING                                                   $
$                                                                      $
$$$$$$$$$$$$$$$$$$$$$$$$$$$$$$$$$$$$$$$$$$$$$$$$$$$$$$$$$$$$$$$$$$$$$$$$
ALTER    220 $                                                         $
PARAM     // C,N,NOP / V,N,MINUS1=-1 $                                 $
$$$$$$$$$$$$$$$$$$$$$$$$$$$$$$$$$$$$$$$$$$$$$$$$$$$$$$$$$$$$$$$$$$$$$$$$
$                                                                      $
$  THE BELOW ALTER PARAMETER BY THE NAME OF (NFRQM1) MUST BE SET BY    $
$  THE USER.  NFRQM1 MUST HAVE A VALUE EQUAL TO THE NUMBER OF          $
$  FREQUENCIES COMPUTED MINUS ONE; FOR EXAMPLE, IF THE NUMBER OF       $
$  FREQUENCIES EQUALS TO 2, THEN NFRQM1=1.  THIS CONTROLS THE NUMBER   $
$  OF TIMES THE ELEMENT STRAIN ENERGY LOOP IS EXECUTED.                $
$                                                                      $
PARAM     // C,N,NOP / V,N,NFRQM1=1 $     <<<--- THIS MUST BE SET BY USER $
$                                                                      $
$$$$$$$$$$$$$$$$$$$$$$$$$$$$$$$$$$$$$$$$$$$$$$$$$$$$$$$$$$$$$$$$$$$$$$$$
LABEL     ESEDYN $                                                     $
PARTN     UPVC,CP, / UPVC1,,UPVC2, / C,N,1 $                           $
PARTN     QPC,CP, / QPC1,,QPC2, / C,N,1 $                              $
GPFDR     CASECC,UPVC1,KELM,KDICT,ECT,EQEXIN,GPECT,,QPC1 /             $
          ONRGY1,OGPFB1 / C,N,STATICS $                                $
OFP       ONRGY1,OGPFB1,,,, // $                                       $
PARTN     CP,,RP / ,CP1,, / C,N,1 $                                    $
PARTN     RP,,CP / ,RP1,, / C,N,1 $                                    $
EQUIV     UPVC2,UPVC / MINUS1 $                                        $
EQUIV     QPC2,QPC / MINUS1 $                                          $
EQUIV     CP1,CP / MINUS1 $                                            $
EQUIV     RP1,RP / MINUS1 $                                            $
REPT      ESEDYN,NFRQM1 $                                              $
ENDALTER $                                                             $
$$$$$$$$$$$$$$$$$$$$$$$$$$$$$$$$$$$$$$$$$$$$$$$$$$$$$$$$$$$$$$$$$$$$$$$$
$                                                                      $
$  CASE CONTROL INPUT REQUIRED                                         $
$      ELEMENT STRAIN ENERGY OUTPUT REQUEST:                           $
$                        ESE=ALL                                       $
$               OR.      ESE=N                 (WHERE N IS A SET NUMBER) $
$                                                                      $
$  BULK DATA INPUT REQUIRED                                            $
$      DMI        WHERE NFREQ IS THE NUMBER OF FREQUENCIES COMPUTED    $
$                 (NFREQ=NFRQM1+1). TWO DMI MATRICES MUST BE INPUT     $
$                 AS FOLLOWS:                                          $
$                        CP   -  MUST BE A 1-COLUMN BY NFREQ-ROW MATRIX. $
$                                THE FIRST ROW=0., ALL OTHER ROWS=1.   $
$                        RP   -  MUST BE A 1-COLUMN BY NFREQ-ROW MATRIX. $
$                                ALL ROWS=1., EXCEPT FOR LAST ROW=0.   $
$                                                                      $
$$$$$$$$$$$$$$$$$$$$$$$$$$$$$$$$$$$$$$$$$$$$$$$$$$$$$$$$$$$$$$$$$$$$$$$$
$$$$$$$$$$$$$$$$$$$$$$$$$$$$$$$$$$$$$$$$$$$$$$$$$$$$$$$$$$$$$$$$$$$$$$$$
CEND
TITLE= ELASTIC LINE MODEL OF THE AH-1G HELICOPTER
SUBTITLE= UNDAMPED FORCED RESPONSE STRAIN ENERGY METHOD
LABEL= PILOT SEAT RESPONSE TO 1000 LB 2/REV VERT HUB SHEAR
ECHO=BOTH
FREQ=10
OUTPUT
   DISP(SORT1,REAL)=ALL
   ESE=ALL
DLOAD=1000
BEGIN BULK
```

GRID	1		39.50	0.0	50.0				
GRID	2		46.0	0.0	50.0				
GRID	3		61.25	0.0	50.0				
GRID	4		75.0	0.0	50.0				
GRID	5		75.5	0.0	29.0				20MM GUN
GRID	6		93.0	0.0	50.0				
GRID	7		113.5	0.0	50.0				
GRID	8		131.5	0.0	50.0				PILOT
GRID	9		140.0	0.0	50.0				
GRID	10		148.5	0.0	50.0				
GRID	11		190.0	0.0	50.0				
GRID	12		197.0	0.0	50.0				
GRID	13		213.0	0.0	50.0				
GRID	14		250.0	0.0	50.0				
GRID	15		277.0	0.0	50.0				
GRID	16		299.57	0.0	49.59				
GRID	17		317.72	0.0	50.72				
GRID	18		338.61	0.0	52.01				
GRID	19		359.51	0.0	53.31				
GRID	20		380.42	0.0	54.61				
GRID	21		401.33	0.0	55.90				
GRID	22		422.24	0.0	57.20				
GRID	23		443.15	0.0	58.50				
GRID	24		464.10	0.0	59.80				
GRID	25		480.23	0.0	75.40				
GRID	26		488.93	0.0	83.82				
GRID	27		497.77	0.0	92.37				
GRID	28		506.60	0.0	100.91				
GRID	29		515.43	0.0	109.46				
GRID	30		520.67	0.0	118.27				
GRID	31		520.67	7.20	118.27				
GRID	32		520.67	14.10	118.27				T/R HUB
GRID	33		199.8588	-60.0	62.246				
GRID	34		196.575	-42.5	61.226				
GRID	35		194.230	-30.0	60.498				
GRID	36		192.202	-19.19	59.868				
GRID	37		192.202	19.19	59.868				
GRID	38		194.230	30.0	60.498				
GRID	39		196.575	42.5	61.226				
GRID	40		199.8588	60.0	62.246				
GRID	41		189.94	-12.375	77.57				
GRID	42		189.94	12.375	77.57				
GRID	43		211.72	-12.375	77.57				
GRID	44		211.72	12.375	77.57				
GRID	45		214.50	0.0	77.57				
GRID	46		189.94	-12.375	77.57				
GRID	47		189.94	12.375	77.57				
GRID	48		211.72	-12.375	77.57				
GRID	49		211.72	12.375	77.57				
GRID	50		214.50	0.0	77.57				
GRID	51		200.	0.0	83.8				XMSN
GRID	52		200.	0.0	77.2				
GRID	53		200.	0.0	98.0				
GRID	54		200.	0.0	115.0				
GRID	55		200.	0.0	153.0				M/R HUB
GRID	60		248.0	0.0	86.0				ENGINE
CBAR	12	12	1	2	0.0	1.0	0.0	1	
CBAR	23	23	2	3	0.0	1.0	0.0	1	
CBAR	34	34	3	4	0.0	1.0	0.0	1	
CRIGD1	45	4	5						
CBAR	46	46	4	6	0.0	1.0	0.0	1	
CBAR	67	67	6	7	0.0	1.0	0.0	1	
CBAR	78	78	7	8	0.0	1.0	0.0	1	
CBAR	89	89	8	9	0.0	1.0	0.0	1	
CBAR	910	910	9	10	0.0	1.0	0.0	1	
CBAR	1011	1011	10	11	0.0	1.0	0.0	1	
CBAR	1112	1112	11	12	0.0	1.0	0.0	1	
CBAR	1213	1213	12	13	0.0	1.0	0.0	1	
CBAR	1314	1314	13	14	0.0	1.0	0.0	1	
CBAR	1415	1415	14	15	0.0	1.0	0.0	1	
CBAR	1516	1516	15	16	0.0	1.0	0.0	1	
CBAR	1617	1617	16	17	0.0	1.0	0.0	1	
CBAR	1718	1718	17	18	0.0	1.0	0.0	1	
CBAR	1819	1819	18	19	0.0	1.0	0.0	1	
CBAR	1920	1920	19	20	0.0	1.0	0.0	1	
CBAR	2021	2021	20	21	0.0	1.0	0.0	1	
CBAR	2122	2122	21	22	0.0	1.0	0.0	1	
CBAR	2223	2223	22	23	0.0	1.0	0.0	1	
CBAR	2324	2324	23	24	0.0	1.0	0.0	1	

```
CBAR     2425     2425     24       25       0.0      1.0      0.0      1
CBAR     2526     2526     25       26       0.0      1.0      0.0      1
CBAR     2627     2627     26       27       0.0      1.0      0.0      1
CBAR     2728     2728     27       28       0.0      1.0      0.0      1
CBAR     2829     2829     28       29       0.0      1.0      0.0      1
CBAR     2930     2930     29       30       0.0      1.0      0.0      1        +2930
+2930                      0.0      0.0      0.0      -1.57    0.0      -5.21
CBAR     3031     3031     30       31       1.0      0.0      0.0      1        +3031
+3031    56
CBAR     3132     3132     31       32       1.0      0.0      0.0      1
CRIGD2   30310    30       31       13
CBAR     3334     3334     33       34       1.0      0.0      0.0      1
CBAR     3435     3435     34       35       1.0      0.0      0.0      1
CBAR     3536     3536     35       36       1.0      0.0      0.0      1
CBAR     3612     3612     36       12       1.0      0.0      0.0      1        +3612
+3612                      0.0      0.0      0.0      -4.798   0.0      9.868
CBAR     1237     1237     12       37       1.0      0.0      0.0      1        +1237
+1237                      -4.798   0.0      9.868    0.0      0.0      0.0
CBAR     3738     3738     37       38       1.0      0.0      0.0      1
CBAR     3839     3839     38       39       1.0      0.0      0.0      1
CBAR     3940     3940     39       40       1.0      0.0      0.0      1
CRIGD1   1240     12       41       42       43       44       45
CRIGD1   5140     51       46       47       48       49       50
CBAR     5112     5112     51       12       0.0      1.0      0.0      1        +LIFTLNK
+LIFTLNK                   -3.10    0.0      -7.90    -0.1     0.0      16.15
CELAS1   41461    1        41       1        46       1
CELAS1   41462    2        41       2        46       2
CELAS1   41463    3        41       3        46       3
CELAS1   42471    1        42       1        47       1
CELAS1   42472    2        42       2        47       2
CELAS1   42473    3        42       3        47       3
CELAS1   43481    1        43       1        48       1
CELAS1   43482    2        43       2        48       2
CELAS1   43483    3        43       3        48       3
CELAS1   44491    1        44       1        49       1
CELAS1   44492    2        44       2        49       2
CELAS1   44493    3        44       3        49       3
CELAS1   45503    33       45       3        50       3
CRIGD2   515253   51       52       123456   53       12
CBAR     5253     5253     52       53       0.0      1.0      0.0      1        +5253
+5253    56
CBAR     5354     5354     53       54       0.0      1.0      0.0      1
CBAR     5455     5455     54       55       0.0      1.0      0.0      1
CRIGD1   1460     14       60
PBAR     12       1        1000.    1650.    250.     200.
PBAR     23       1        1000.    3300.    700.     200.
PBAR     34       1        1000.    5350.    1100.    200.
PBAR     46       1        1000.    5800.    1100.    225.
PBAR     67       1        1000.    7300.    2750.    850.
PBAR     78       1        1000.    7300.    3000.    850.
PBAR     89       1        1000.    7300.    3200.    850.
PBAR     910      1        1000.    9750.    8200.    2000.
PBAR     1011     1        1000.    12750.   14710.   3250.
PBAR     1112     1        1000.    18000.   14710.   3150.
PBAR     1213     1        1000.    18000.   14710.   3150.
PBAR     1314     1        1000.    13900.   11670.   2900.
PBAR     1415     1        1000.    12100.   10400.   2650.
PBAR     1516     1        1000.    8850.    9300.    2100.
PBAR     1617     1        42.7403  5138.39  6244.61  3326.62
PBAR     1718     1        47.4632  4686.89  6300.05  2387.82
PBAR     1819     1        41.4892  3376.80  4650.61  1863.98
PBAR     1920     1        38.7424  2797.46  3323.30  1422.92
PBAR     2021     1        37.5606  2419.04  2301.92  1113.34
PBAR     2122     1        36.7154  1919.77  1782.38  881.70
PBAR     2223     1        34.7744  1418.76  1322.74  634.50
PBAR     2324     1        35.5467  1008.00  1159.10  428.36
PBAR     2425     1        38.50    182.6    5150.    113.5
PBAR     2526     1        35.13    168.0    1900.    81.2
PBAR     2627     1        32.70    152.0    1620.    69.0
PBAR     2728     1        30.25    135.0    1540.    56.8
PBAR     2829     1        27.85    100.0    1060.    43.5
PBAR     2930     1        25.45    72.0     650.     43.7
PBAR     3031     1        1000.    5.5      5.5      11.0
PBAR     3132     1        1000.    3.5      3.5      7.0
PBAR     3334     1        1000.    2600.    454.     230.
PBAR     3435     1        1000.    4250.    1041.    380.
PBAR     3536     1        1000.    8250.    1485.    560.
PBAR     3612     1        1000.    9912.    1693.    5150.
PBAR     1237     1        1000.    9912.    1683.    5150.
```

```
PBAR    3738    1       1000.   8250.   1485.   560.
PBAR    3839    1       1000.   4250.   1031.   380.
PBAR    3940    1       1000.   2600.   454.    270.
PBAR    5112    1       25.81
PELAS   1       28125.
PELAS   2       28125.
PELAS   3       4500.
PELAS   33      20000.
PBAR    5253    1       100.    72.     72.     144.
PBAR    5354    1       100.    135.    135.    270.
PBAR    5455    1       100.    120.    120.    240.
MAT1    1       1.0+6   1.0+6
CONM2   1       1               12.029
CONM2   2       2               34.965
CONM2   3       3               66.882
CONM2   4       4               198.829
CONM2   5       5               253.4
CONM2   6       6               439.371
CONM2   7       7               551.594
CONM2   8       8               355.019
CONM2   9       9               189.893
CONM2   10      10              714.319
CONM2   11      11              686.484
CONM2   12      12              125.393                                 +MT12
+MT12   0.849+6
CONM2   13      13              836.348
CONM2   14      14              554.022
CONM2   15      15              296.573
CONM2   16      16              87.781
CONM2   17      17              33.058
CONM2   18      18              43.977
CONM2   19      19              60.541
CONM2   20      20              41.474
CONM2   21      21              48.633
CONM2   22      22              22.713
CONM2   23      23              15.102
CONM2   24      24              44.152
CONM2   25      25              19.136
CONM2   26      26              6.809
CONM2   27      27              11.934
CONM2   28      28              8.475
CONM2   29      29              4.968
CONM2   30      30              2.544
CONM2   300     30              25.994
CONM2   31      31              11.282
CONM2   32      32              34.066
CONM2   33      33              9.489
CONM2   34      34              35.704
CONM2   35      35              36.459
CONM2   36      36              95.577
CONM2   37      37              95.577
CONM2   38      38              36.459
CONM2   39      39              35.704
CONM2   40      40              9.489
CONM2   51      51              103.695
CONM2   52      52              115.708
CONM2   53      53              270.518
CONM2   54      54              125.560
CONM2   55      55              33.249
CONM2   550     55              947.5
CONM2   60      60              585.35                                  +ENG
+ENG    17800.          109500.                 94700.
PARAM   WTMASS  .00259
PARAM   GRDPNT  0
FREQ    10      10.7    10.8
RLOAD2  1000    553     0       0       99      0
DAREA   553     55      3       1000.
TABLED1 99                                                              +B(F)
+B(F)   0.0     1.0     200.0   1.0     ENDT
$$$$$$$$$$$$$$$$$$$$$$$$$$$$$$$$$$$$$$$$$$$$$$$$$$$$$$$$$$$$$$$$$$$$$$$$
$  THESE DMI MATRICES MUST BE INPUT FOR ELEMENT DYNAMIC STRAIN ENERGY   $
$  CALCULATIONS - CONSULT ALTER PACKAGE IN EXECUTIVE DECK FOR DETAILS.  $
DMI     CP      0       2       1       1               2       1       $
DMI     CP      1       1       0.      2       1.                      $
DMI     RP      0       2       1       1               2       1       $
DMI     RP      1       1       1.      2       0.                      $
$$$$$$$$$$$$$$$$$$$$$$$$$$$$$$$$$$$$$$$$$$$$$$$$$$$$$$$$$$$$$$$$$$$$$$$$
ENDDATA
END*
```

APPENDIX B

NASTRAN FORCED RESPONSE STRAIN ENERGY OUTPUT DATA

PILOT SEAT RESPONSE TO 1000 LB 2/REV VERT HUB SHEAR

C A S E C O N T R O L D E C K E C H O

```
CARD
COUNT
  1      TITLE= ELASTIC LINE MODEL OF THE AH-1G HELICOPTER
  2      SUBTITLE= UNDAMPED FORCED RESPONSE STRAIN ENERGY METHOD
  3      LABEL= PILOT SEAT RESPONSE TO 1000 LB 2/REV VERT HUB SHEAR
  4      ECHO=BOTH
  5      FREQ=10
  6      OUTPUT
  7         DISP=S(PRTI,REAL<=ALL
  8         ESE=ALL
  9      DLOAD=1000
 10      BEGIN BULK
```

PILOT SEAT RESPONSE TO 1000 LB 2/REV VERT HUB SHAK

INPUT BULK DATA DECK ECHO

. 1 ..	2 ..	3 ..	4 ..	5 ..	6 ..	7 ..	8 ..	9 ..	10 .	
GRID	1		33.50	0.0	50.0					
GRID	2		46.0	0.0	50.0					
GRID	3		61.25	0.0	50.0					
GRID	4		75.0	0.0	50.0					
GRID	5		75.5	0.0	69.0					20MM GUN
GRID	6		94.0	0.0	50.0					
GRID	7		113.5	0.0	50.0					
GRID	8		141.5	0.0	50.0					PILOT
GRID	9		140.0	0.0	50.0					
GRID	10		148.5	0.0	50.0					
GRID	11		190.0	0.0	50.0					
GRID	12		197.0	0.0	50.0					
GRID	13		213.0	0.0	50.0					
GRID	14		250.0	0.0	50.0					
GRID	15		277.0	0.0	50.0					
GRID	16		279.57	0.0	49.59					
GRID	17		317.72	0.0	50.72					
GRID	18		338.61	0.0	52.01					
GRID	19		359.51	0.0	53.41					
GRID	20		380.42	0.0	54.61					
GRID	21		401.23	0.0	55.90					
GRID	22		422.24	0.0	57.20					
GRID	23		443.15	0.0	58.50					
GRID	24		464.10	0.0	59.80					
GRID	25		480.23	0.0	75.40					
GRID	26		488.93	0.0	83.82					
GRID	27		497.77	0.0	92.37					
GRID	28		506.60	0.0	100.91					
GRID	29		515.43	0.0	109.46					
GRID	30		520.67	0.0	118.27					
GRID	31		520.67	7.70	118.27					
GRID	32		520.67	14.10	118.27					T/R HUB
GRID	33		199.858	-60.0	62.246					
GRID	34		196.375	-42.5	61.226					
GRID	35		194.230	-30.0	60.428					
GRID	36		192.202	-19.19	59.868					
GRID	37		192.202	19.19	59.868					
GRID	38		194.230	30.0	60.428					
GRID	39		196.575	42.5	61.226					
GRID	40		199.858	60.0	62.246					
GRID	41		189.94	-12.375	77.57					
GRID	42		189.94	12.375	77.57					
GRID	43		211.72	-12.375	77.57					
GRID	44		211.72	12.375	77.57					
GRID	45		214.50	0.0	77.57					
GRID	46		189.94	-12.375	77.57					
GRID	47		189.94	12.375	77.57					
GRID	48		211.72	-12.375	77.57					
GRID	49		211.72	12.375	77.57					
GRID	50		214.50	0.0	77.57					
GRID	51		200.	0.0	81.40					XMSN
GRID	52		200.	0.0	77.62					
GRID	53		200.	0.0	96.0					
GRID	54		200.	0.0	115.0					
GRID	55		200.	0.0	134.0					M/R HUB
GRID	60		248.0	0.0	88.0					ENGINE
CBAR	12	12	1	2	0.0	1.0	0.0	1		
CBAR	23	23	2	3	0.0	1.0	0.0	1		
CBAR	34	34	3	4	0.0	1.0	0.0	1		
CBAR	45	45	4	5						
CBAR	56	46	4	6	0.0	1.0	0.0	1		
CBAR	67	67	6	7	0.0	1.0	0.0	1		
CBAR	78	78	7	8	0.0	1.0	0.0	1		
CBAR	89	89	8	9	0.0	1.0	0.0	1		
CBAR	910	910	9	10	0.0	1.0	0.0	1		
CBAR	1011	1011	10	11	0.0	1.0	0.0	1		
CBAR	1112	1112	11	12	0.0	1.0	0.0	1		
CBAR	1213	1213	12	13	0.0	1.0	0.0	1		
CBAR	1314	1314	13	14	0.0	1.0	0.0	1		
CBAR	1415	1415	14	15	0.0	1.0	0.0	1		
CBAR	1516	1516	15	16	0.0	1.0	0.0	1		
CBAR	1617	1617	16	17	0.0	1.0	0.0	1		

PILOT SEAT RESPONSE TO 1000 LB 2/REV VERT HUB SHEAR

INPUT BULK DATA DECK ECHO

1	2	3	4	5	6	7	8	9	10
CBAR	1718	1718	17	18	0.0	1.0	0.0	1	
CBAR	1819	1819	18	19	0.0	1.0	0.0	1	
CBAR	1920	1920	19	20	0.0	1.0	0.0	1	
CBAR	2021	2021	20	21	0.0	1.0	0.0	1	
CBAR	2122	2122	21	22	0.0	1.0	0.0	1	
CBAR	2223	2223	22	23	0.0	1.0	0.0	1	
CBAR	2324	2324	23	24	0.0	1.0	0.0	1	
CBAR	2425	2425	24	25	0.0	1.0	0.0	1	
CBAR	2526	2526	25	26	0.0	1.0	0.0	1	
CBAR	2627	2627	26	27	0.0	1.0	0.0	1	
CBAR	2728	2728	27	28	0.0	1.0	0.0	1	
CBAR	2829	2829	28	29	0.0	1.0	0.0	1	
CBAR	2930	2930	29	30	0.0	1.0	0.0	1	&2930
&2930			0.0	0.0	0.0	-1.57	0.0	-5.21	
CBAR	3031	3031	30	31	1.0	0.0	0.0	1	&3031
&3031	56								
CBAR	3132	3132	31	32	1.0	0.0	0.0	1	
CRIGD2	30310	30	31	13					
CBAR	3334	3334	33	34	1.0	0.0	0.0	1	
CBAR	3435	3435	34	35	1.0	0.0	0.0	1	
CBAR	3536	3536	35	36	1.0	0.0	0.0	1	
CBAR	3612	3612	36	12	1.0	0.0	0.0	1	&3612
&3612			0.0	0.0	0.0	-4.798	0.0	9.868	
CBAR	1237	1237	12	37	1.0	0.0	0.0	1	&1237
&1237			-4.798	0.0	9.868	0.0	0.0	0.0	
CBAR	3738	3738	37	38	1.0	0.0	0.0	1	
CBAR	3839	3839	38	39	1.0	0.0	0.0	1	
CBAR	3940	3940	39	40	1.0	0.0	0.0	1	
CRIGD1	1240	12	41	42	43	44	45		
CRIGD1	5140	51	46	47	48	49	50		
CBAR	5112	5112	51	12	0.0	1.0	0.0	1	&LIFTLNK
&LIFTLNK			-3.10	0.0	-7.90	-0.1	0.0	16.15	
CELAS1	41461	1	41	1	46	1			
CELAS1	41462	2	41	2	46	2			
CELAS1	41463	3	41	3	46	3			
CELAS1	42471	1	42	1	47	1			
CELAS1	42472	2	42	2	47	2			
CELAS1	42473	3	42	3	47	3			
CELAS1	43481	1	43	1	48	1			
CELAS1	43482	2	43	2	48	2			
CELAS1	43483	3	43	3	48	3			
CELAS1	44491	1	44	1	49	1			
CELAS1	44492	2	44	2	49	2			
CELAS1	44493	3	44	3	49	3			
CELAS1	45503	33	45	3	50	3			
CRIGD2	515253	51	52	123456	53	12			
CBAR	5253	5253	52	53	0.0	1.0	0.0	1	&5253
&5253	56								
CBAR	5354	5354	53	54	0.0	1.0	0.0	1	
CBAR	5455	5455	54	55	0.0	1.0	0.0	1	
CRIGD1	1460	14	60						
PBAR	12	1	1000.	1650.	250.	200.			
PBAR	23	1	1000.	3300.	700.	200.			
PBAR	34	1	1000.	5350.	1100.	200.			
PBAR	46	1	1000.	5800.	1100.	225.			
PBAR	67	1	1000.	7300.	2750.	850.			
PBAR	78	1	1000.	7300.	3000.	850.			
PBAR	89	1	1000.	7300.	3200.	850.			
PBAR	910	1	1000.	9750.	5200.	2000.			
PBAR	1011	1	1000.	12750.	14710.	3250.			
PBAR	1112	1	1000.	14000.	14710.	3150.			
PBAR	1213	1	1000.	15000.	14710.	3150.			
PBAR	1314	1	1000.	13400.	11670.	2900.			
PBAR	1415	1	1000.	12100.	10400.	2650.			
PBAR	1516	1	1000.	9650.	9300.	2100.			
PBAR	1617	1	42.7403	5138.39	6244.61	3326.62			
PBAR	1718	1	47.4032	4506.52	6400.05	2307.82			
PBAR	1819	1	41.4882	3376.80	4650.61	1963.28			
PBAR	1920	1	39.7424	2797.46	3823.30	1425.92			
PBAR	2021	1	27.3505	2419.04	2301.92	1113.34			
PBAR	2122	1	26.7134	1919.77	1752.35	841.70			
PBAR	2223	1	34.7744	1418.76	1422.74	634.59			

PILOT SEAT RESPONSE TO 1000 LH 2/REV VERT HUB SHEAR

INPUT BULK DATA DECK ECHO

```
*  1  **  2  **  3  **  4  **  5  **  6  **  7  **  8  **  9  ** 10  *
PBAR    2324       1          35.5467 1008.00 1159.10 428.36
PBAR    2425       1          38.50   1826.6  5150.   113.5
PBAR    2526       1          35.13   168.0   1900.   81.2
PBAR    2627       1          32.70   152.0   1620.   69.0
PBAR    2728       1          30.25   135.0   1540.   56.8
PBAR    2829       1          27.85   100.0   1060.   48.5
PBAR    2930       1          25.45   72.0    650.    43.7
PBAR    3031       1          1000.   5.5     5.5     11.0
PBAR    3132       1          1000.   3.5     3.5     7.0
PBAR    3334       1          1000.   2600.   454.    230.
PBAR    3435       1          1000.   4250.   1031.   380.
PBAR    3536       1          1000.   8250.   1485.   560.
PBAR    3612       1          1000.   9912.   1683.   5150.
PBAR    1237       1          1000.   9912.   1683.   5150.
PBAR    3738       1          1000.   8250.   1485.   560.
PBAR    3839       1          1000.   4250.   1031.   380.
PBAR    3940       1          1000.   2600.   454.    230.
PBAR    5112       1          25.81
PELAS   1          28125.
PELAS   2          28125.
PELAS   3          4500.
PELAS   33         20000.
PBAR    5253       1          100.    72.     72.     144.
PBAR    5354       1          100.    135.    135.    270.
PBAR    5455       1          100.    120.    120.    240.
MAT1    1          1.0E6      1.0E6
CONM2   1          1                  12.029
CONM2   2          2                  34.985
CONM2   3          3                  86.882
CONM2   4          4                  198.829
CONM2   5          5                  253.4
CONM2   6          6                  439.371
CONM2   7          7                  551.594
CONM2   8          8                  355.019
CONM2   9          9                  189.893
CONM2   10         10                 714.319
CONM2   11         11                 686.484
CONM2   12         12                 125.393                        GWT12
GWT12   0.8409.6
CONM2   13         13                 836.348
CONM2   14         14                 554.022
CONM2   15         15                 296.573
CONM2   16         16                 87.781
CONM2   17         17                 33.058
CONM2   18         18                 43.977
CONM2   19         19                 60.541
CONM2   20         20                 41.474
CONM2   21         21                 48.633
CONM2   22         22                 22.713
CONM2   23         23                 15.102
CONM2   24         24                 44.152
CONM2   25         25                 19.136
CONM2   26         26                 6.809
CONM2   27         27                 11.934
CONM2   28         28                 8.475
CONM2   29         29                 4.468
CONM2   30         30                 2.544
CONM2   300        30                 25.974
CONM2   31         31                 11.282
CONM2   32         32                 30.066
CONM2   33         33                 9.489
CONM2   34         34                 35.704
CONM2   35         35                 36.459
CONM2   36         36                 35.577
CONM2   37         37                 35.577
CONM2   38         38                 36.459
CONM2   39         39                 35.704
CONM2   40         40                 9.489
CONM2   41         41                 103.193
CONM2   42         42                 113.705
CONM2   43         43                 270.513
CONM2   44         44                 130.960
```

PLOT 1 AT RESPONSE TO 1000 LB 78EV VERT HUB SHEAR

INPUT BULK DATA DECK ECHO

```
*   1  ..   2  ..   3  ..   4  ..   5  ..   6  ..   7  ..   8  ..   9  .. 10  .
CONM1   55      55              33.240
CONM2   560     55              947.5
CONM2   60      60              38.35
GENG    17800.          109500.                 94300.                  &ENG
PARAM   WTMASS  .00259
PARAM   GRDPNT  0
EIGR    10      10.7    10.8
RLOAD1  1000    553     0       0       99      0
DAREA   553     55      3       1000.
TABLED1 99
&ENDT   0.0     1.0     200.0   1.0     ENDT                            &ENDT
$$$$$$$$$$$$$$$$$$$$$$$$$$$$$$$$$$$$$$$$$$$$$$$$$$$$$$$$$$$$$$$$$$$$$$$$$$$$
$  THESE DMI MATRICES MUST BE INPUT FOR ELEMENT DYNAMIC STRAIN ENERGY    $
$  CALCULATIONS - CONSULT ALTER PACKAGE IN EXECUTIVE DECK FOR DETAILS.    $
DMI     CP      0       2       1       1                       2       1       $
DMI     CP      1       1       0.      2       1.                      $
DMI     RP      0       2       1       1                       2       1       $
DMI     RP      1       1       1.      2       0.                      $
$$$$$$$$$$$$$$$$$$$$$$$$$$$$$$$$$$$$$$$$$$$$$$$$$$$$$$$$$$$$$$$$$$$$$$$$$$$$
ENDDATA
```

TOTAL COUNT= 236

*** USER INFORMATION MESSAGE 207, BULK DATA NOT SORTED,XSORT WILL RE-ORDER DECK.

PILOT SEAT RESPONSE TO 1000 LB 2/REV VERT HUB SHEAR

S O R T E D B U L K D A T A E C H O

CARD COUNT	1	2	3	4	5	6	7	8	9	10
1-	CBAR	12	12	1	2	.0	1.0	.0	1	
2-	CBAR	23	23	2	3	.0	1.0	.0	1	
3-	CBAR	34	34	3	4	.0	1.0	.0	1	
4-	CBAR	46	46	4	6	.0	1.0	.0	1	
5-	CBAR	67	67	6	7	.0	1.0	.0	1	
6-	CBAR	78	78	7	8	.0	1.0	.0	1	
7-	CBAR	89	89	8	9	.0	1.0	.0	1	
8-	CBAR	910	910	9	10	.0	1.0	.0	1	
9-	CBAR	1011	1011	10	11	.0	1.0	.0	1	
10-	CBAR	1112	1112	11	12	.0	1.0	.0	1	
11-	CBAR	1213	1213	12	13	.0	1.0	.0	1	
12-	CBAR	1237	1237	12	37	1.0	.0	.0	1	G1237
13-	G1237			-4.798	0.0	9.869	0.0	0.0	0.0	
14-	CBAR	1314	1314	13	14	.0	1.0	.0	1	
15-	CBAR	1415	1415	14	15	.0	1.0	.0	1	
16-	CBAR	1516	1516	15	16	.0	1.0	.0	1	
17-	CBAR	1617	1617	16	17	.0	1.0	.0	1	
18-	CBAR	1718	1718	17	18	.0	1.0	.0	1	
19-	CBAR	1819	1819	18	19	.0	1.0	.0	1	
20-	CBAR	1920	1920	19	20	.0	1.0	.0	1	
21-	CBAR	2021	2021	20	21	.0	1.0	.0	1	
22-	CBAR	2122	2122	21	22	.0	1.0	.0	1	
23-	CBAR	2223	2223	22	23	.0	1.0	.0	1	
24-	CBAR	2324	2324	23	24	.0	1.0	.0	1	
25-	CBAR	2425	2425	24	25	.0	1.0	.0	1	
26-	CBAR	2526	2526	25	26	.0	1.0	.0	1	
27-	CBAR	2627	2627	26	27	.0	1.0	.0	1	
28-	CBAR	2728	2728	27	28	.0	1.0	.0	1	
29-	CBAR	2929	2829	28	29	.0	1.0	.0	1	
30-	CBAR	2930	2930	29	30	.0	1.0	.0	1	G2930
31-	G2930			0.0	0.0	0.0	-1.57	0.0	-5.21	
32-	CBAR	3031	3031	30	31	1.0	.0	.0	1	G3031
33-	G3031	56								
34-	CBAR	3132	3132	31	32	1.0	.0	.0	1	
35-	CBAR	3334	3334	33	34	1.0	.0	.0	1	
36-	CBAR	3435	3435	34	35	1.0	.0	.0	1	
37-	CBAR	3536	3536	35	36	1.0	.0	.0	1	
38-	CBAR	3612	3612	36	12	1.0	.0	.0	1	G3612
39-	G3612			0.0	0.0	0.0	-4.798	0.0	9.868	
40-	CBAR	3738	3738	37	38	1.0	.0	.0	1	
41-	CBAR	3839	3839	38	39	1.0	.0	.0	1	
42-	CBAR	3940	3940	39	40	1.0	.0	.0	1	
43-	CBAR	5112	5112	51	12	.0	1.0	.0	1	GLIFTLNK
44-	GLIFTLNK			-3.10	0.0	-7.90	-0.1	0.0	16.15	
45-	CBAR	5253	5253	52	53	.0	1.0	.0	1	G5253
46-	G5253	56								
47-	CBAR	5354	5354	53	54	.0	1.0	.0	1	
48-	CBAR	5455	5455	54	55	.0	1.0	.0	1	
49-	CELAS1	41461	1	41	1	46	1			
50-	CELAS1	41462	2	41	2	46	2			
51-	CELAS1	41463	3	41	3	46	3			
52-	CELAS1	42471	1	42	1	47	1			
53-	CELAS1	42472	2	42	2	47	2			
54-	CELAS1	42473	3	42	3	47	3			
55-	CELAS1	43481	1	43	1	48	1			
56-	CELAS1	43482	2	43	2	48	2			
57-	CELAS1	43483	3	43	3	48	3			
58-	CELAS1	44491	1	44	1	49	1			
59-	CELAS1	44492	2	44	2	49	2			
60-	CELAS1	44493	3	44	3	49	3			
61-	CELAS1	45503	31	45	3	50	3			
62-	CONM2	1	1		1.+029					
63-	CONM2	2	2		34.055					
64-	CONM2	3	3		85.042					
65-	CONM2	4	4		1.+029					
66-	CONM2	5	5		2.+4					
67-	CONM2	6	6		4.+4.371					
68-	CONM2	7	7		1.+4.994					
69-	CONM2	8	8		2.+4.61					
70-	CONM2	9	9		1.+4.21					
71-	CONM2	10	10		71.+4.1					
72-	CONM2	11	11		4.+4					

PILOT SEAT RESPONSE TO 1000 LB 2/REV VERT HUB SHEAR

S O R T E D B U L K D A T A E C H O

CARD COUNT	1	2	3	4	5	6	7	8	9	10
73-	CONM2	12	12		129.393					GWT12
74-	GWT12	0.84966								
75-	CONM2	13	13		836.348					
76-	CONM2	14	14		554.022					
77-	CONM2	15	15		296.573					
78-	CONM2	16	16		87.781					
79-	CONM2	17	17		33.058					
80-	CONM2	18	18		43.977					
81-	CONM2	19	19		60.541					
82-	CONM2	20	20		41.474					
83-	CONM2	21	21		48.633					
84-	CONM2	22	22		22.713					
85-	CONM2	23	23		15.102					
86-	CONM2	24	24		44.152					
87-	CONM2	25	25		19.136					
88-	CONM2	26	26		6.809					
89-	CONM2	27	27		11.934					
90-	CONM2	28	28		8.475					
91-	CONM2	29	29		4.368					
92-	CONM2	30	30		2.544					
93-	CONM2	31	31		11.282					
94-	CONM2	32	32		34.066					
95-	CONM2	33	33		9.489					
96-	CONM2	34	34		35.704					
97-	CONM2	35	35		36.459					
98-	CONM2	36	36		95.577					
99-	CONM2	37	37		95.577					
100-	CONM2	38	38		36.459					
101-	CONM2	39	39		35.704					
102-	CONM2	40	40		9.489					
103-	CONM2	51	51		103.895					
104-	CONM2	52	52		115.708					
105-	CONM2	53	53		270.518					
106-	CONM2	54	54		126.560					
107-	CONM2	55	55		33.249					
108-	CONM2	60	60		585.35					GENG
109-	GENG	17800.		109500.		94300.				
110-	CONM2	300	30		25.994					
111-	CONM2	550	55		947.5					
112-	CRIGD1	45	4	5						
113-	CRIGD1	1240	12	41	42	43	44	45		
114-	CRIGD1	1460	14	60						
115-	CRIGD1	5140	51	46	47	48	49	50		
116-	CRIGD2	30310	30	31	13					
117-	CRIGD3	515253	51	52	123456	53	12			
118-	DAREA	553	55	3	1000.					
119-	DMI	CP	0	2	1	1		2	1	$
120-	DMI	CP	1	1	0.0	2	1.			$
121-	DMI	RP	0	2	1	1		2	1	$
122-	DMI	RP	1	1	1.	2	0.0			$
123-	FREQ	10	10.7	10.8						
124-	GRID	1		39.50	.0	50.0				
125-	GRID	2		46.0	.0	50.0				
126-	GRID	3		61.25	.0	50.0				
127-	GRID	4		75.0	.0	50.0				
128-	GRID	5		75.5	.0	29.0				20MM GUN
129-	GRID	6		93.0	.0	50.0				
130-	GRID	7		113.5	.0	50.0				
131-	GRID	8		131.5	.0	50.0				PILOT
132-	GRID	9		140.0	.0	50.0				
133-	GRID	10		148.5	.0	50.0				
134-	GRID	11		190.0	.0	50.0				
135-	GRID	12		197.0	.0	50.0				
136-	GRID	13		213.0	.0	50.0				
137-	GRID	14		250.0	.0	50.0				
138-	GRID	15		277.0	.0	50.0				
139-	GRID	16		244.57	.0	43.59				
140-	GRID	17		317.72	.0	56.72				
141-	GRID	18		339.61	.0	52.01				
142-	GRID	19		350.51	.0	53.11				
143-	GRID	20		371.42	.0	54.61				
144-	GRID	21		401.33	.0	55.90				

PILOT SEAT RESPONSE TO 1000 LB 2/REV VERT HUB SHEAR

S O R T E D B U L K D A T A E C H O

CARD COUNT	1	2	3	4	5	6	7	8	9	10	
145-	GRID	22		422.24	.0	57.20					
146-	GRID	23		442.15	.0	58.50					
147-	GRID	24		464.10	.0	59.80					
148-	GRID	25		480.23	.0	75.40					
149-	GRID	26		488.93	.0	84.52					
150-	GRID	27		497.77	.0	92.37					
151-	GRID	28		506.60	.0	100.91					
152-	GRID	29		515.43	.0	109.46					
153-	GRID	30		520.67	.0	118.27					
154-	GRID	31		520.67	7.20	118.27					
155-	GRID	32		520.67	14.10	118.27					T/R HUB
156-	GRID	33		193.858	-60.0	62.246					
157-	GRID	34		196.575	-42.5	61.226					
158-	GRID	35		194.230	-30.0	60.498					
159-	GRID	36		192.202	-19.19	59.868					
160-	GRID	37		192.202	19.19	59.868					
161-	GRID	38		194.230	30.0	60.498					
162-	GRID	39		196.575	42.5	61.226					
163-	GRID	40		199.858	60.0	62.246					
164-	GRID	41		189.94	-12.375	77.57					
165-	GRID	42		189.94	12.375	77.57					
166-	GRID	43		211.72	-12.375	77.57					
167-	GRID	44		211.72	12.375	77.57					
168-	GRID	45		214.50	.0	77.57					
169-	GRID	46		189.94	-12.375	77.57					
170-	GRID	47		189.94	12.375	77.57					
171-	GRID	48		211.72	-12.375	77.57					
172-	GRID	49		211.72	12.375	77.57					
173-	GRID	50		214.50	.0	77.57					
174-	GRID	51		200.	.0	83.8					XMSN
175-	GRID	52		200.	.0	77.2					
176-	GRID	53		200.	.0	98.0					
177-	GRID	54		200.	.0	115.0					
178-	GRID	55		200.	.0	153.0					M/R HUB
179-	GRID	60		248.0	.0	86.0					ENGINE
180-	MAT1	1	1.066	1.066							
181-	PARAM	GRDPNT	0								
182-	PARAM	WTMASS	.00259								
183-	PBAR	12	1	1000.	1650.	250.	200.				
184-	PBAR	23	1	1000.	3300.	700.	200.				
185-	PBAR	34	1	1000.	5350.	1100.	200.				
186-	PBAR	46	1	1000.	5800.	1100.	225.				
187-	PBAR	57	1	1000.	7300.	2750.	850.				
188-	PBAR	78	1	1000.	7300.	3000.	850.				
189-	PBAR	89	1	1000.	7300.	3200.	850.				
190-	PBAR	910	1	1000.	9750.	8200.	2000.				
191-	PBAR	1011	1	1000.	12750.	14710.	3250.				
192-	PBAR	1112	1	1000.	18000.	14710.	3150.				
193-	PBAR	1213	1	1000.	18000.	14710.	3150.				
194-	PBAR	1237	1	1000.	9912.	1683.	5150.				
195-	PBAR	1314	1	1000.	13000.	11670.	2900.				
196-	PBAR	1415	1	1000.	12100.	10400.	2650.				
197-	PBAR	1516	1	1000.	8850.	9300.	2100.				
198-	PBAR	1617	1	42.7403	5138.39	6244.61	3326.62				
199-	PBAR	1718	1	47.4632	4936.89	6300.05	2387.82				
200-	PBAR	1819	1	41.4892	3376.80	4650.61	1863.98				
201-	PBAR	1920	1	39.7424	2797.46	3323.30	1422.92				
202-	PBAR	2021	1	37.5605	2419.04	2301.92	1113.34				
203-	PBAR	2122	1	36.7154	1919.77	1782.38	881.70				
204-	PBAR	2223	1	38.7744	1418.76	1322.74	634.50				
205-	PBAR	2324	1	37.5407	1008.00	1159.10	429.36				
206-	PBAR	2425	1	38.50	182.6	5150.	113.5				
207-	PBAR	2526	1	31.13	163.0	1300.	81.2				
208-	PBAR	2627	1	42.70	152.0	1620.	69.0				
209-	PBAR	2728	1	40.25	135.0	1340.	56.8				
210-	PBAR	2829	1	27.85	100.0	1060.	48.5				
211-	PBAR	2930	1	25.45	72.0	650.	43.7				
212-	PBAR	3031	1	1000.	5.5	5.5	11.0				
213-	PBAR	3132	1	1000.	5.5	5.5	7.0				
214-	PBAR	4334	1	1000.	2600.	454.	230.				
215-	PBAR	4435	1	1000.	4250.	1041.	390.				
216-	PBAR	4536	1	1000.	4250.	1045.	590.				

PILOT SEAT RESPONSE TO 1000 LB 22REV VERT HUB SHEAR

S O R T E D B U L K D A T A E C H O

CARD COUNT	1	2	3	4	5	6	7	8	9	10
217-	PBAR	3612	1	1000.	9912.	1683.	5150.			
218-	PBAR	3738	1	1000.	8250.	1485.	560.			
219-	PBAR	3839	1	1000.	4250.	1031.	380.			
220-	PBAR	3940	1	1000.	2600.	454.	230.			
221-	PBAR	5112	1	25.81						
222-	PBAR	5253	1	100.	72.	72.	144.			
223-	PBAR	5354	1	100.	135.	135.	270.			
224-	PBAR	5455	1	100.	120.	120.	240.			
225-	PELAS	1	28125.							
226-	PELAS	2	28125.							
227-	PELAS	3	4500.							
228-	PELAS	33	20000.							
229-	RLOAD2	1000	553	0	0	99	0			
230-	TABLED1	99								CB%EC
231-	CB%EC	0.0	1.0	200.0	1.0	ENDT				
	ENDDATA									

PILOT SEAT RESPONSE TO 1000 LB 2/REV VERT HUB SHEAR

LEVEL 2.0 NASTRAN DMAP COMPILER - SOURCE LISTING

```
OPTIONS IN EFFECT@  GO      ERR=2   NOLIST  NODECK  NOREF   NOOSCAR

  1  BEGIN    NO.9 DIRECT FREQUENCY RESPONSE ANALYSIS - SERIES N $
  2  FILE     KGGX#TAPE/ KGG#TAPE/ GOD#SAVE/ GMD#SAVE $
  3  GP1      GEOM1,GEOM2,/GPL,EQEXIN,GPDT,CSTM,BGPDT,SIL/V,N,LUSET/  V,N,
              NOGPDT $
  4  SAVE     LUSET,NOGPDT $
  5  PURGE    USET,GM,GO,KAA,BAA,MAA,K4AA,KFS,PSF,QPC,EST,ECT,PLTSETX,PLTPAR,
              GPSETS,ELSETS/NOGPDT $
  6  CHKPNT   GPL,EQEXIN,GPDT,CSTM,BGPDT,SIL,USET,GM,GO,KAA,BAA,MAA,K4AA,
              KFS,PSF,QPC,EST,ECT,PLTSETX,PLTPAR,GPSETS,ELSETS $
  7  COND     LBL5,NOGPDT $
  8  GP2      GEOM2,EQEXIN/ECT $
  9  CHKPNT   ECT $
 10  PARAML   PCDB//C,N,PRES/C,N,/C,N,/C,N,/V,N,NOPCDB $
 11  PURGE    PLTSETX,PLTPAR,GPSETS,ELSETS/NOPCDB $
 12  COND     P1,NOPCDB $
 13  PLTSET   PCDB,EQEXIN,ECT/PLTSETX,PLTPAR,GPSETS,ELSETS/V,N,NSIL/   V,N,
              JUMPPLOT#-1 $
 14  SAVE     NSIL,JUMPPLOT $
 15  PRTMSG   PLTSETX// $
 16  PARAM    //C,N,MPY/V,N,PLTFLG/C,N,1/C,N,1 $
 17  PARAM    //C,N,MPY/V,N,PFILE/C,N,0/C,N,0 $
 18  COND     P1,JUMPPLOT $
 19  PLOT     PLTPAR,GPSETS,ELSETS,CASECC,BGPDT,EQEXIN,SIL,,,,/PLOTX1/   V,N,
              NSIL/V,N,LUSET/V,N,JUMPPLOT/V,N,PLTFLG/V,N,PFILE $
 20  SAVE     PFILE $
 21  PRTMSG   PLOTX1//$
 22  LABEL    P1 $
 23  CHKPNT   PLTPAR,GPSETS,ELSETS $
 24  GP3      GEOM3,EQEXIN,GEOM2/,GPTT/V,N,NOGRAV $
 25  CHKPNT   GPTT $
 26  TA1      ECT,EPT,BGPDT,SIL,GPTT,CSTM/EST,GEI,GPECT,/V,N,LUSET/   V,N,
              NOSIMP#-1/C,N,1/V,N,NOGENL#-1/V,N,GENEL $
 27  SAVE     NOSIMP,NOGENL,GENEL $
 28  [illegible] KAGG,GOST,[illegible],KANN,KAFF,KAAA,MNN,[illegible],MAA,BNN,BFF,BAA,
              KGGX/NOSIMP/[illegible]/GENEL $
 29  CHKPNT   EST,GPECT,GEI,[illegible],KANN,KAFF,KAAA,
              MNN,MFF,MAA,BNN,BFF,BAA $
 30  COND     LBL1,NOSIMP $
```

PILOT SEAT RESPONSE TO 1000 LB Z/REV VERT HUB SHEAR

LEVEL 2.0 NASTRAN DMAP COMPILER - SOURCE LISTING

```
31  PARAM     //C,N,ADD/V,N,NOKGGX/C,N,1/C,N,0 $
32  PARAM     //C,N,ADD/V,N,NOMGG/C,N,1/C,N,0 $
33  PARAM     //C,N,ADD/V,N,NOBGG/-1/C,N,1/C,N,0 $
34  PARAM     //C,N,ADD/V,N,NOK4GG/C,N,1/C,N,0 $
35  EMA       EST,CSTM,MPT,DIT,GEOM2,/KELM,KDICT,MELM,MDICT,BELM,BDICT/   V,
              N,NOKGGX/V,N,NOMGG/V,N,NOBGG/V,N,NOK4GG/C,N,/C,Y,COUPMASS/C,Y,
              CPBAR/C,Y,CPROD/C,Y,CPQUAD1/C,Y,CPQUAD2/C,Y,CPTRIA1/C,Y,
              CPTRIA2/C,Y,CPTUBE/C,Y,CPQDPLT/C,Y,CPTRPLT/C,Y,CPTRMSC $
36  SAVE      NOKGGX,NOMGG,NOBGG,NOK4GG $
37  CHKPNT    KELM,KDICT,MELM,MDICT,BELM,BDICT $
38  COND      LBLKGGX,NOKGGX $
39  EMA       GPECT,KDICT,KELM/KGGX,GPST $
40  CHKPNT    KGGX,GPST $
41  LABEL     LBLKGGX $
42  COND      LBLMGG,NOMGG $
43  EMA       GPECT,MDICT,MELM/MGG,/C,N,-1/C,Y,WTMASS/1.0 $
44  CHKPNT    MGG $
45  LABEL     LBLMGG $
46  COND      LBLBGG,NOBGG $
47  EMA       GPECT,BDICT,BELM/BGG, $
48  CHKPNT    BGG $
49  LABEL     LBLBGG $
50  COND      LBLK4GG,NOK4GG $
51  EMA       GPECT,KDICT,KELM/K4GG,/V,N,NOK4GG $
52  CHKPNT    K4GG $
53  LABEL     LBLK4GG $
54  PURGE     MNN,MFF,MAA/NOMGG $
55  PURGE     BNN,BFF,BAA/NOBGG $
56  CHKPNT    MGG,MNN,MFF,MAA,BGG,BNN,BFF,BAA $
57  COND      LBL1,GRDPNT $
58  COMB      ERROR4,NOMGG $
59  GPWG      BGPDT,CSTM,EQEXIN,MGG/OGPWG/V,Y,GRDPNT/-1/C,Y,WTMASS $
60  OFP       OGPWG,,,,,// $
61  LABEL     LBL1 $
62  EQUIV     KGGX,KGG/NOGENL $
63  CHKPNT    KGG $
64  COND      LBL11,NOGENL $
65  SMA1      GPL,KGGX/SIGG/V,N,LUSET/V,N,NOGENL/V,N,JUSTIFY $
```

PILOT SEAT RESPONSE TO 1000 LB 2/REV VERT HUB SHEAR

LEVEL 2.0 NASTRAN DMAP COMPILER - SOURCE LISTING

```
 66  CHKPNT   KGG $
 67  LABEL    LBL11 $
 68  PARAM    //C,N,MPY/V,N,NSKIP/C,N,0/C,N,0 $
 69  GP4      CASECC,GEOM4,EQEXIN,SIL,GPDT,BGPDT,CSTM/RG,,USET,ASET/  V,N,
              LUSET/V,N,MPCF1/V,N,MPCF2/V,N,SINGLE/V,N,OMIT/V,N,REACT/V,N,
              NSKIP/V,N,REPEAT/V,N,NOSET/V,N,NOL/V,N,NOA/C,Y,SUBID $
 70  SAVE     MPCF1,SINGLE,OMIT,NOSET,REACT,MPCF2,NSKIP,REPEAT,NOL,NOA $
 71  PURGE    GM,GMD/MPCF1/GO,GOD/OMIT/KFS,PSF,QPC/SINGLE $
 72  CHKPNT   GM,GMD,RG,GO,GOD,KFS,PSF,QPC,USET $
 73  COND     LBL4,GENEL $
 74  COND     LBL4,NOSIMP $
 75  GPSP     GPL,GPST,USET,SIL/OGPST/V,N,NOGPST $
 76  SAVE     NOGPST $
 77  COND     LBL4,NOGPST $
 78  OFP      OGPST,,,,,// $
 79  LABEL    LBL4 $
 80  EQUIV    KGG,KNN/MPCF1/MGG,MNN/MPCF1/ BGG,BNN/MPCF1/K4GG,K4NN/MPCF1 $
 81  CHKPNT   KNN,MNN,BNN,K4NN $
 82  COND     LBL2,MPCF1 $
 83  MCE1     USET,RG/GM $
 84  CHKPNT   GM $
 85  MCE2     USET,GM,KGG,MGG,BGG,K4GG/KNN,MNN,BNN,K4NN $
 86  CHKPNT   KNN,MNN,BNN,K4NN $
 87  LABEL    LBL2 $
 88  EQUIV    KNN,KFF/SINGLE/MNN,MFF/SINGLE/BNN,BFF/SINGLE/K4NN,K4FF/SINGLE $
 89  CHKPNT   KFF,MFF,BFF,K4FF $
 90  COND     LBL3,SINGLE $
 91  SCE1     USET,KNN,MNN,BNN,K4NN/KFF,KFS,,MFF,BFF,K4FF $
 92  CHKPNT   KFS,KFF,MFF,BFF,K4FF $
 93  LABEL    LBL3 $
 94  EQUIV    KFF,KAA/OMIT $
 95  EQUIV    MFF,MAA/OMIT $
 96  EQUIV    BFF,BAA/OMIT $
 97  EQUIV    K4FF,K4AA/OMIT $
 98  CHKPNT   KAA,MAA,BAA,K4AA $
 99  COND     LBL5,OMIT $
100  SMP1     USET,KFF,,,/GO,KAA,KOO,LOO,,,,, $
```

PILOT AT RESPONSE TO 1000 LB 2/REV VERT HUB SHEAR

LEVEL 2.0 NASTRAN DMAP COMPILER - SOURCE LISTING

```
101  CHKPNT   GO,KAA $
102  COND     LBLM,NOMGG $
103  SMP2     USET,GO,MFF/MAA $
104  CHKPNT   MAA $
105  LABEL    LBLM $
106  COND     LBLB,NOBGG $
107  SMP2     USET,GO,BFF/BAA $
108  CHKPNT   BAA $
109  LABEL    LBLB $
110  COND     LBL5,NOK4GG $
111  SMP2     USET,GO,K4FF/K4AA $
112  CHKPNT   K4AA $
113  LABEL    LBL5 $
114  DPD      DYNAMICS,GPL,SIL,USET/GPLD,SILD,USETD,TFPOOL,DLT,PSDL,FRL,,,,
              EQDYN/V,N,LUSET/V,N,LUSETD/V,N,NOTFL/V,N,NODLT/V,N,NOPSDL/V,N,
              NOFRL/V,N,NONLFT/V,N,NOTRL/V,N,NOEED/C,N,/V,N,NOUE $
115  SAVE     LUSETD,NOUE,NODLT,NOFRL,NOPSDL $
116  EQUIV    GO,GOD/NOUE/GM,GMD/NOUE $
117  CHKPNT   USETD,EQDYN,TFPOOL,DLT,FRL,GOD,GMD,SILD,PSDL,GPLD $
118  PARAM    //C,N,ADD/V,N,NEVER/C,N,1/C,N,0 $
119  PARAM    //C,N,MPY/V,N,REPEATE/C,N,-1/C,N,1 $
120  MAG      MATPOOL,BGPDT,EQEXIN,CSTM/BDPOOL/V,N,NOKBFL/V,N,NOABFL/ V,N,
              MFACT $
121  SAVE     MFACT,NOKBFL,NOABFL $
122  PARAM    //C,N,AND/V,N,NOFL/V,N,NOABFL/V,N,NOKBFL $
123  PURGE    KBFL/NOKBFL/ ABFL/NOABFL $
124  COND     LBLFL3,NOFL $
125  MTRXIN,  ,BDPOOL,EQDYN,,/ABFL,KBFL,/V,N,LUSETD/V,N,NOABFL/V,N,NOKBFL/C,
              N,0 $
126  SAVE     NOABFL,NOKBFL $
127  LABEL    LBLFL3 $
128  CHKPNT   ABFL,KBFL $
129  PARAM    //C,N,MPY/V,N,CARDNO/C,N,0/C,N,0 $
130  JUMP     LBL13 $
131  LABEL    LBL13 $
132  PURGE    OUDVC1,OUDVC2,XYPLTFA,OPPC1,OQPC1,OUPVC1,OESC1,OEFC1,OPPC2,
              OQPC2,OUPVC2,OESC2,OEFC2,XYPLTF,PSDF,AUTO,XYPLTR,   K2PP,M2PP,
              B2PP,K2DD,M2DD,B2DD/NEVER $
133  CASE     CASECC,PSDL/CASEXX/C,N,FREQ/V,N,REPEATE/V,N,NOLOOP $
```

PILOT SEAT RESPONSE TO 1000 LB 2/REV VERT HUB SHEAR

LEVEL 2.0 NASTRAN DMAP COMPILER - SOURCE LISTING

```
134  SAVE      REPEATF,NOLOOP $
135  CHKPNT    CASEXX $
136  MTRXIN    CASEXX,MATPOOL,EQUYN,,TFPOOL/K2PP,M2PP,B2PP/V,N,LUSETD/V,N,
               NOK2PP/V,N,NOM2PP/V,N,NOB2PP $
137  SAVE      NOK2PP,NOM2PP,NOB2PP $
138  PARAM     //C,N,AND/V,N,NOM2PP/V,N,NOABFL/V,N,NOM2PP $
139  PARAM     //C,N,AND/V,N,NOK2PP/V,N,NOFL /V,N,NOK2PP $
140  EQUIV     M2PP,M2PP/NOABFL $
141  ADDS      ABFL,KBFL,K2PP,,/K2PP/C,N,X-1.0,0.0< $
142  COND      LBLFL2,NOABFL $
143  TRNSP     ABFL/ABFLT $
144  ADD       ABFLT,M2PP/M2PP/V,N,MFACT $
145  LABEL     LBLFL2 $
146  PARAM     //C,N,AND/V,N,NOEBA/V,N,NOUE/V,N,NOB2PP $
147  PARAM     //C,N,AND/V,N,KDEK2/V,N,NOGENL/V,N,NOSIMP $
148  PARAM     //C,N,AND/V,N,MDEMA/V,N,NOUE/V,N,NOM2PP $
149  PURGE     K2DD/NOK2PP/M2DD/NOM2PP/B2DD/NOB2PP $
150  EQUIV     M2PP,M2DD/NOA/B2PP,B2DD/NOA/K2PP,K2DD/NOA/MAA,MDD/MDEMA/BAA,
               BDD/BDEMA $
151  CHKPNT    K2PP,M2PP,B2PP,K2DD,M2DD,B2DD,BDD,MDD $
152  COND      LBL18,NOGPDT $
153  XSAD      USETD,GM,GO,KAA,BAA,MAA,K4AA,K2PP,M2PP,B2PP/KDD,BDD,MDD,GMD,
               GOD,K2DD,M2DD,B2DD/C,N,FREQRESP/C,N,DISP/C,N,DIRECT/C,Y,G=0.0/
               C,N,0.0/C,N,0.0/V,N,NOK2PP/V,N,NOM2PP/V,N,NOB2PP/   V,N,MPCFIT/
               V,N,SINGLE/V,N,OMIT/V,N,NOUE/V,N,NOKAGG/V,N,NOMGG/V,N,KDEK2/C,
               N,-1 $
154  LABEL     LBL18 $
155  EQUIV     B2DD,BDD/NOMGG/ M2DD,MDD/NOSIMP/ K2DD,KDD/KDEK2 $
156  CHKPNT    KDD,BDD,MDD,GMD,GOD $
157  COND      ERROR1,NOFRL $
158  COND      ERROR2,NODLT $
159  FBMS      CASEXX,USETD,SLT,FRL,GMD,GOD,KDD,BDD,MDD,,DLT/UDVF,PSF,PDF,PDF/
               C,N,DISP/C,N,DIRECT/V,N,LUSETD/V,N,MPCFIT/V,N,SINGLE/V,N,OMIT/
               V,N,NONCUP/V,N,FROSET $
160  EQUIV     PDF,PDF/NOSET $
161  CHKPNT    PSF,PDF,UDVF,PDF $
162  VDR       CASEXX,EQUYN,USETD,UDVF,PDF,XYCDB,/UDVCT,/C,N,FREQRESP/C,N,
               DIRECT/V,N,PPOINTS/V,N,NOD/V,N,NOD/C,N,0 $
163  SAVE      NOD,NOD,NOSORT2 $
164  COND      LBL15,NOD $
165  FBPD      LBL15A,NOSORT2 $
```

```
166  CHKPNT   OUDVC1 $
167  SDR3     OUDVC1,,,,,/OUDVC2,,,,, $
168  OFP      OUDVC2,,,,,//V,N,CARDNO $
169  SAVE     CARDNO $
170  CHKPNT   OUDVC2 $
171  XYTRAN   XYCDB,OUDVC2,,,,/XYPLTFA/C,N,FREQ/C,N,DSET/V,N,PFILE/V,N,
              CARDNO $
172  SAVE     PFILE,CARDNO $
173  XYPLOT   XYPLTFA// $
174  JUMP     LBL15 $
175  LABEL    LBL15A $
176  OFP      OUDVC1,,,,,//V,N,CARDNO $
177  SAVE     CARDNO $
178  LABEL    LBL15 $
179  COND     LBL16,NOP $
180  EQUIV    UDVF,UPVC/NOA $
181  COND     LBL19,NOA $
182  SDR1     USETD,,UDVF,,,GOD,GMD,PSF,KFS,,/UPVC,,OPC/C,N,1/C,N,DYNAMICS $
183  LABEL    LBL19 $
184  CHKPNT   UPVC,OPC $
185  SDR2     CASEXX,CSTM,MPT,DIT,EQDYN,SILD,,,,PPF,OPC,UPVC,EST,XYCDB,PPF/
              OPPC1,OOPC1,OUPVC1,OESC1,OEFC1,/C,N,FREQRESP/V,N,NOSORT2 $
186  SAVE     NOSORT2 $
187  COND     LBL17,NOSORT2 $
188  SDR3     OPPC1,OOPC1,OUPVC1,OESC1,OEFC1,/OPPC2,OOPC2,OUPVC2,OESC2,
              OEFC2, $
189  CHKPNT   OPPC2,OOPC2,OUPVC2,OESC2,OEFC2 $
190  OFP      OPPC2,OOPC2,OUPVC2,OEFC2,OESC2,,//V,N,CARDNO $
191  SAVE     CARDNO $
192  XYTRAN   XYCDB,OPPC2,OOPC2,OUPVC2,OESC2,OEFC2/XYPLTF/C,N,FREQ/C,N,DSET/
              V,N,PFILE/V,N,CARDNO $
193  SAVE     PFILE,CARDNO $
194  XYPLOT   XYPLTF// $
195  COND     LBL16,NOPSDL $
196  RANDOM   XYCDB,DIT,PSDL,OUPVC2,OPPC2,OOPC2,OESC2,OEFC2,CASEXX/PSDF,AUTO/
              V,N,NORD $
197  SAVE     NORD $
198  CHKPNT   PSDF,AUTO $
199  COND     LBL16,NORD $
```

```
200  XYTRAN   XYCDB,PSDF,AUTO,,,/XYPLTR/C,N,RAND/C,N,PSET/V,N,PFILE/   V,N,
              CARDNO $
201  SAVE     PFILE,CARDNO $
202  XYPLOT   XYPLTR// $
203  JUMP     LBL16 $
204  LABEL    LBL17 $
205  OFP      OUPVC1,OPPC1,OQPC1,OEFC1,OESC1,//V,N,CARDNO $
206  SAVE     CARDNO $
207  LABEL    LBL16 $
208  COND     FINIS,REPEATF $
209  REPT     LBL13,100 $
210  JUMP     ERROR3 $
211  JUMP     FINIS $
212  LABEL    ERROR3 $
213  PRTPARM  //C,N,-3/C,N,DIRERRD $
214  LABEL    ERROR2 $
215  PRTPARM  //C,N,-2/C,N,DIRERRD $
216  LABEL    ERROR1 $
217  PRTPARM  //C,N,-1/C,N,DIRERRD $
218  LABEL    ERROR4 $
219  PRTPARM  //C,N,-4/C,N,DIRERRD $
220  LABEL    FINIS $
220  PARAM    // C,N,NOD / V,N,MINUS1#-1 $
220  PARAM    // C,N,NOD / V,N,NFROM1#1 $     <<<--- THIS MUST BE SET BY USER
220  LABEL    ESEDYN $
220  PARTN    UPVC,CP, / UPVC1,,UPVC2, / C,N,1 $
220  PARTN    QPC,CP, / QPC1,,QPC2, / C,N,1 $
220  GPFDR    CASECC,UPVC1,KELM,KDICT,ECT,EQEXIN,GPECT,,QPC1 /
              UNRGY1,QGPFB1 / C,N,STATICS $
220  OFP      UNRGY1,QGPFB1,,,, // $
220  PARTN    CP,,RP / ,CP1,, / C,N,1 $
220  PARTN    RP,,CP / ,RP1,, / C,N,1 $
220  EQUIV    UPVC2,UPVC / MINUS1 $
220  EQUIV    QPC2,QPC / MINUS1 $
220  EQUIV    CP1,CP / MINUS1 $
220  EQUIV    RP1,RP / MINUS1 $
220  REPT     ESEDYN,NFROM1 $
```

201 END $

NO ERRORS FOUND - EXECUTE NASTRAN PROGRAM

*** SYSTEM INFORMATION MESSAGE 3113, EMGPRO PROCESSING DOUBLE PRECISION ELEMENTS OF TYPE 34 STARTING WITH ID 12
*** SYSTEM INFORMATION MESSAGE 3107, EMGOLD IS PROCESSING ELEMENTS OF TYPE # 34, BEGINNING WITH ELEMENT ID # 12
*** SYSTEM INFORMATION MESSAGE 3113, EMGPRO PROCESSING DOUBLE PRECISION ELEMENTS OF TYPE 11 STARTING WITH ID 41461
*** SYSTEM INFORMATION MESSAGE 3113, EMGPRO PROCESSING DOUBLE PRECISION ELEMENTS OF TYPE 30 STARTING WITH ID 1
*** SYSTEM INFORMATION MESSAGE 3107, EMGOLD IS PROCESSING ELEMENTS OF TYPE # 30, BEGINNING WITH ELEMENT ID # 1

*** USER WARNING MESSAGE 3041

EXTERNAL GRID POINT 0 DOES NOT EXIST OR IS NOT A GEOMETRIC GRID POINT.
THE BASIC ORIGIN WILL BE USED.

PILOT SEAT RESPONSE TO 1000 LB 2/REV VERT HUB SHEAR

OUTPUT FROM GRID POINT WEIGHT GENERATOR

REFERENCE POINT = 0

MO - RIGID BODY MASS MATRIX IN BASIC COORDINATE SYSTEM

8.393988E+03	0.0	0.0	0.0	5.764303E+05	-5.615605E+02
0.0	8.393988E+03	0.0	-5.764303E+05	0.0	1.620686E+06
0.0	0.0	8.393988E+03	5.615605E+02	-1.620686E+06	0.0
0.0	-5.764303E+05	5.615605E+02	5.097202E+07	-2.923877E+05	-1.165462E+08
5.764303E+05	0.0	-1.620686E+06	-2.923877E+05	4.145019E+08	-6.641581E+04
-5.615605E+02	1.620686E+06	0.0	-1.165462E+08	-6.641581E+04	3.650629E+08

S - TRANSFORMATION MATRIX FOR SCALAR MASS PARTITION

1.000000E+00	0.0	0.0
0.0	1.000000E+00	0.0
0.0	0.0	1.000000E+00

DIRECTION MASS AXIS SYSTEM (S)	MASS	X-C.G.	Y-C.G.	Z-C.G.
X	8.393988E+03		6.690031E-02	6.867180E+01
Y	8.393988E+03	1.930770E+02		6.867180E+01
Z	8.393988E+03	1.930770E+02	6.690031E-02	

I(S) - INERTIAS RELATIVE TO C.G.

1.138809E+07	1.839634E+05	5.250832E+06
1.839634E+05	6.200066E+07	2.785246E+04
5.250832E+06	2.785246E+04	5.214592E+07

I(Q) - PRINCIPLE INERTIAS

1.072188E+07		
	5.281123E+07	
		6.200149E+07

Q - TRANSFORMATION MATRIX -- I(Q) = QT*I(S)*Q

9.920564E-01	-1.257325E-01	4.100546E-03
-3.433208E-03	5.523831E-03	9.999790E-01
-1.257525E-01	-9.920404E-01	5.048282E-03

*** USER WARNING MESSAGE 3017
ONE OR MORE POTENTIAL SINGULARITIES HAVE NOT BEEN REMOVED BY SINGLE OR MULTI-POINT CONSTRAINTS.

PILOT SEAT RESPONSE TO 1000 LB 2/REV VERT HUB SHEAR

G R I D P O I N T S I N G U L A R I T Y T A B L E SPC 0 MPC 0

POINT ID.	TYPE	SINGULARITY ORDER	LIST OF COORDINATE COMBINATIONS THAT WILL REMOVE SINGULARITY STRONGEST COMBINATION	WEAKER COMBINATION	WEAKEST COMBINATION
51	G	2	2 3	2 1	
51	G	2	4 6		

***USER INFORMATION MESSAGE 3023--PARAMETERS FOR SYMMETRIC DECOMPOSITION OF DATA BLOCK SCRATCH8 X N # 254 <
TIME ESTIMATE# 1 C AVG # 18 PC AVG # 0 SPILL GROUPS # 0 S AVG # 1
ADDITIONAL CORE# -60050 C MAX # 29 PCMAX # 0 PC GROUPS # 0 PREFACE LOOPS # 1

ELASTIC LINE MODEL OF THE AH-1G HELICOPTER APRIL 4, 1979 NASTRAN 1/17/77 PAGE 23
UNDAMPED FORCED RESPONSE STRAIN ENERGY METHOD

PILOT SEAT RESPONSE TO 1000 LB 2/REV VERT HUB SHEAR
FREQUENCY # 1.070000E+01

C O M P L E X   D I S P L A C E M E N T   V E C T O R
(REAL/IMAGINARY)

POINT ID.	TYPE	T1	T2	T3	R1	R2	R3
1	G	4.879033E-05	7.594489E-04	2.246049E-03	-1.990273E-05	8.833830E-05	-7.553022E-06
		0.0	0.0	0.0	0.0	0.0	0.0
2	G	4.879029E-05	7.103570E-04	1.671908E-03	-1.990273E-05	8.831159E-05	-7.551654E-06
		0.0	0.0	0.0	0.0	0.0	0.0
3	G	4.878988E-05	5.952902E-04	3.263431E-04	-1.990273E-05	8.810051E-05	-7.534421E-06
		0.0	0.0	0.0	0.0	0.0	0.0
4	G	4.878883E-05	4.918925E-04	-8.830251E-04	-1.990273E-05	8.776944E-05	-7.499312E-06
		0.0	0.0	0.0	0.0	0.0	0.0
5	G	-1.794369E-03	7.018571E-05	-9.269097E-04	-1.990273E-05	8.776944E-05	-7.499312E-06
		0.0	0.0	0.0	0.0	0.0	0.0
6	G	4.888122E-05	3.578712E-04	-2.444029E-03	-2.025251E-05	8.584579E-05	-7.370015E-06
		0.0	0.0	0.0	0.0	0.0	0.0
7	G	4.898130E-05	2.094217E-04	-4.205648E-03	-2.035795E-05	8.642823E-05	-7.072649E-06
		0.0	0.0	0.0	0.0	0.0	0.0
8	G	4.906347E-05	8.615702E-05	-5.788453E-03	-2.045055E-05	9.021643E-05	-6.582316E-06
		0.0	0.0	0.0	0.0	0.0	0.0
9	G	4.910053E-05	3.152138E-05	-6.568957E-03	-2.049426E-05	9.368551E-05	-6.263381E-06
		0.0	0.0	0.0	0.0	0.0	0.0
10	G	4.913666E-05	-2.054669E-05	-7.373322E-03	-2.051285E-05	9.569622E-05	-5.980552E-06
		0.0	0.0	0.0	0.0	0.0	0.0
11	G	4.929608E-05	-2.396884E-04	-1.159485E-02	-2.056868E-05	1.105516E-04	-4.449787E-06
		0.0	0.0	0.0	0.0	0.0	0.0
12	G	4.932020E-05	-2.700204E-04	-1.238336E-02	-2.057839E-05	1.148687E-04	-4.214764E-06
		0.0	0.0	0.0	0.0	0.0	0.0
13	G	4.878275E-05	-3.328014E-04	-1.429697E-02	-1.918181E-05	1.229342E-04	-3.621753E-06
		0.0	0.0	0.0	0.0	0.0	0.0
14	G	4.816464E-05	-4.312445E-04	-1.880680E-02	-1.567381E-05	1.141520E-04	-1.676149E-06
		0.0	0.0	0.0	0.0	0.0	0.0
15	G	4.602459E-05	-4.536966E-04	-2.150857E-02	-1.249643E-05	8.489643E-05	8.613956E-09
		0.0	0.0	0.0	0.0	0.0	0.0
16	G	1.718699E-05	-4.373363E-04	-2.307774E-02	-9.257573E-06	5.398045E-05	1.816951E-06
		0.0	0.0	0.0	0.0	0.0	0.0
17	G	3.508163E-05	-3.724010E-04	-2.371792E-02	-7.470569E-06	1.649327E-05	4.270445E-06
		0.0	0.0	0.0	0.0	0.0	0.0
18	G	7.997074E-06	-2.445758E-04	-2.362421E-02	-4.543251E-06	-2.538796E-05	7.184965E-06
		0.0	0.0	0.0	0.0	0.0	0.0
19	G	-6.532741E-05	-5.185393E-05	-2.252059E-02	-7.866381E-07	-7.989637E-05	1.086060E-05
		0.0	0.0	0.0	0.0	0.0	0.0
20	G	-2.019676E-04	2.101635E-04	-2.009551E-02	4.185483E-06	-1.511985E-04	1.490726E-05
		0.0	0.0	0.0	0.0	0.0	0.0
21	G	-5.449943E-04	5.632807E-04	-1.594215E-02	1.059630E-05	-2.444503E-04	1.912507E-05
		0.0	0.0	0.0	0.0	0.0	0.0
22	G	-9.509423E-04	9.946288E-04	-9.700246E-03	1.873024E-05	-3.500714E-04	2.387170E-05
		0.0	0.0	0.0	0.0	0.0	0.0
23	G	-1.522225E-03	1.523443E-03	-1.084047E-03	3.008498E-05	-4.704958E-04	2.963022E-05
		0.0	0.0	0.0	0.0	0.0	0.0
24	G	-2.230321E-03	2.172195E-03	9.990390E-03	4.701066E-05	-5.876156E-04	3.695504E-05
		0.0	0.0	0.0	0.0	0.0	0.0

AT RESPONSE TO 1060 LB 2/REV VERT HUB SHEAR
AY = 1.070000E+01

C O M P L E X D I S P L A C E M E N T V E C T O R
(REAL/IMAGINARY)

ID.	TYPE	T1	T2	T3	R1	R2	R3
26	G	-1.140940E-02 0.0	2.006275E-03 0.0	1.956331E-02 0.0	1.132648E-04 0.0	-6.027790E-04 0.0	9.704020E-05 0.0
27	G	-1.666694E-02 0.0	1.882784E-03 0.0	2.490530E-02 0.0	1.633473E-04 0.0	-6.240611E-04 0.0	1.422335E-04 0.0
28	G	-2.207655E-02 0.0	1.726395E-03 0.0	3.051125E-02 0.0	2.232180E-04 0.0	-6.429157E-04 0.0	1.962540E-04 0.0
29	G	-2.762711E-02 0.0	1.533802E-03 0.0	3.625273E-02 0.0	2.956700E-04 0.0	-6.562183E-04 0.0	2.620050E-04 0.0
30	G	-3.326784E-02 0.0	1.295013E-03 0.0	4.210117E-02 0.0	3.806902E-04 0.0	-6.667869E-04 0.0	3.369232E-04 0.0
31	G	-3.918472E-02 0.0	-4.388653E-04 0.0	4.860718E-02 0.0	4.202288E-04 0.0	-6.699718E-04 0.0	3.745395E-04 0.0
32	G	-4.188140E-02 0.0	-4.388669E-04 0.0	4.863283E-02 0.0	4.834172E-04 0.0	-6.699718E-04 0.0	4.290626E-04 0.0
33	G	-4.540849E-02 0.0	-4.388681E-04 0.0	5.262501E-02 0.0	6.261564E-04 0.0	-6.699718E-04 0.0	5.522270E-04 0.0
34	G	1.209431E-03 0.0	-4.540880E-05 0.0	-1.181537E-02 0.0	-1.303410E-05 0.0	1.154802E-04 0.0	-4.102123E-06 0.0
35	G	1.163482E-03 0.0	-4.538610E-05 0.0	-1.166707E-02 0.0	-1.348534E-05 0.0	1.153953E-04 0.0	-4.106071E-06 0.0
36	G	1.130901E-03 0.0	-4.578549E-05 0.0	-1.156893E-02 0.0	-1.424724E-05 0.0	1.152517E-04 0.0	-4.118327E-06 0.0
37	G	1.102926E-03 0.0	-4.673208E-05 0.0	-1.149504E-02 0.0	-1.543707E-05 0.0	1.150277E-04 0.0	-4.138995E-06 0.0
38	G	1.084941E-03 0.0	-4.673173E-05 0.0	-1.229203E-02 0.0	-2.637882E-05 0.0	1.150533E-04 0.0	-4.323740E-06 0.0
39	G	1.384352E-03 0.0	-3.841634E-05 0.0	-1.281920E-02 0.0	-2.776258E-05 0.0	1.153138E-04 0.0	-4.339963E-06 0.0
40	G	1.522702E-03 0.0	-2.801549E-05 0.0	-1.344368E-02 0.0	-2.866358E-05 0.0	1.154839E-04 0.0	-4.358093E-06 0.0
41	G	1.716967E-03 0.0	-1.272978E-05 0.0	-1.433104E-02 0.0	-2.921074E-05 0.0	1.155869E-04 0.0	-4.364634E-06 0.0
42	G	3.164052E-03 0.0	3.270819E-04 0.0	-1.131773E-02 0.0	-2.057839E-05 0.0	1.148687E-04 0.0	-4.214764E-06 0.0
43	G	3.268406E-03 0.0	3.240819E-04 0.0	-1.182705E-02 0.0	-2.057839E-05 0.0	1.148687E-04 0.0	-4.214764E-06 0.0
44	G	3.164092E-03 0.0	2.352843E-04 0.0	-1.381957E-02 0.0	-2.057839E-05 0.0	1.148687E-04 0.0	-4.214764E-06 0.0
45	G	3.268406E-03 0.0	2.352843E-04 0.0	-1.432869E-02 0.0	-2.057839E-05 0.0	1.148687E-04 0.0	-4.214764E-06 0.0
46	G	3.216250E-03 0.0	2.285673E-04 0.0	-1.439356E-02 0.0	-2.057839E-05 0.0	1.148687E-04 0.0	-4.214764E-06 0.0
47	G	3.351126E-03 0.0	3.397190E-04 0.0	-1.268246E-02 0.0	-5.070511E-06 0.0	-9.111081E-05 0.0	-4.252120E-06 0.0
48	G	3.440357E-03 0.0	3.397190E-04 0.0	-1.280796E-02 0.0	-5.070511E-06 0.0	-9.111081E-05 0.0	-4.252120E-06 0.0
49	G	3.351126E-03 0.0	2.471078E-04 0.0	-1.009807E-02 0.0	-5.070511E-06 0.0	-9.111081E-05 0.0	-4.252120E-06 0.0

PILOT SEAT RESPONSE TO 1000 LB 2/REV VERT HUB SHEAR
FREQUENCY = 1.070000E+01

C O M P L E X D I S P L A C E M E N T V E C T O R
%REAL/IMAGINARY%

POINT ID.	TYPE	T1	T2	T3	R1	R2	R3
49	G	3.440352E-03 0.0	2.471078E-04 0.0	-1.082357E-02 0.0	-5.070511E-06 0.0	-9.111081E-05 0.0	-4.252120E-06 0.0
50	G	3.367732E-03 0.0	2.352870E-04 0.0	-1.050753E-02 0.0	-5.070511E-06 0.0	-9.111081E-05 0.0	-4.252120E-06 0.0
51	G	2.820113E-03 0.0	3.285320E-04 0.0	-1.182864E-02 0.0	-5.070511E-06 0.0	-9.111081E-05 0.0	-4.252120E-06 0.0
52	G	3.421443E-03 0.0	2.950665E-04 0.0	-1.182864E-02 0.0	-5.070511E-06 0.0	-9.111081E-05 0.0	-4.252120E-06 0.0
53	G	1.526333E-03 0.0	4.005330E-04 0.0	-1.165854E-02 0.0	4.058259E-07 0.0	-6.140447E-05 0.0	-4.252120E-06 0.0
54	G	7.736734E-04 0.0	3.369586E-04 0.0	-1.151324E-02 0.0	6.826715E-06 0.0	-2.940249E-05 0.0	-4.252120E-06 0.0
55	G	4.579085E-04 0.0	-1.033943E-04 0.0	-1.118203E-02 0.0	1.396899E-05 0.0	2.226951E-06 0.0	-4.252120E-06 0.0
56	G	4.157651E-03 0.0	1.363649E-04 0.0	-1.857850E-02 0.0	-1.567381E-05 0.0	1.141520E-04 0.0	-1.676149E-06 0.0

PILOT SEAT RESPONSE TO 1000 LB 2/REV VERT HUB SHEAR
FREQUENCY # 1.080000E+01

C O M P L E X D I S P L A C E M E N T V E C T O R
%REAL/IMAGINARY%

POINT ID.	TYPE	T1	T2	T3	R1	R2	R3
1	G	3.639970E-05 0.0	7.374098E-04 0.0	1.544747E-03 0.0	-1.934840E-05 0.0	7.904487E-05 0.0	-7.352987E-06 0.0
2	G	3.639965E-05 0.0	6.896183E-04 0.0	1.030996E-03 0.0	-1.934840E-05 0.0	7.902614E-05 0.0	-7.351633E-06 0.0
3	G	3.639935E-05 0.0	5.776007E-04 0.0	-1.733632E-04 0.0	-1.934840E-05 0.0	7.888649E-05 0.0	-7.334588E-06 0.0
4	G	3.639655E-05 0.0	4.769487E-04 0.0	-1.256888E-03 0.0	-1.934840E-05 0.0	7.870367E-05 0.0	-7.299868E-06 0.0
5	G	-1.616378E-03 0.0	6.698249E-05 0.0	-1.296240E-03 0.0	-1.934840E-05 0.0	7.870367E-05 0.0	-7.299868E-06 0.0
6	G	3.648366E-05 0.0	3.465055E-04 0.0	-2.661204E-03 0.0	-1.968848E-05 0.0	7.764685E-05 0.0	-7.172140E-06 0.0
7	G	3.657714E-05 0.0	2.020785E-04 0.0	-4.263084E-03 0.0	-1.979100E-05 0.0	7.915303E-05 0.0	-6.878588E-06 0.0
8	G	3.665465E-05 0.0	8.225408E-05 0.0	-5.725712E-03 0.0	-1.988103E-05 0.0	8.423284E-05 0.0	-6.394771E-06 0.0
9	G	3.668999E-05 0.0	2.919475E-05 0.0	-6.458487E-03 0.0	-1.992354E-06 0.0	8.845895E-05 0.0	-6.080179E-06 0.0
10	G	3.672460E-05 0.0	-2.133229E-05 0.0	-7.219847E-03 0.0	-1.994160E-05 0.0	9.081292E-05 0.0	-5.801274E-06 0.0
11	G	3.688053E-05 0.0	-2.334603E-04 0.0	-1.126373E-02 0.0	-1.999589E-05 0.0	1.069764E-04 0.0	-4.293367E-06 0.0
12	G	3.690472E-05 0.0	-2.627100E-04 0.0	-1.202819E-02 0.0	-2.000833E-05 0.0	1.115734E-04 0.0	-4.062023E-06 0.0
13	G	3.657342E-05 0.0	-3.231217E-04 0.0	-1.389432E-02 0.0	-1.881322E-05 0.0	1.202975E-04 0.0	-3.478511E-06 0.0
14	G	3.579378E-05 0.0	-4.168444E-04 0.0	-1.834191E-02 0.0	-1.511645E-05 0.0	1.434100E-04 0.0	-1.564861E-06 0.0
15	G	3.444219E-05 0.0	-4.366846E-04 0.0	-2.104293E-02 0.0	-1.198728E-05 0.0	8.555621E-05 0.0	9.059426E-08 0.0
16	G	4.299838E-06 0.0	-4.186374E-04 0.0	-2.264039E-02 0.0	-8.735573E-06 0.0	5.560360E-05 0.0	1.865279E-06 0.0
17	G	2.966356E-05 0.0	-3.538299E-04 0.0	-2.332514E-02 0.0	-6.959906E-06 0.0	1.955825E-05 0.0	4.272573E-06 0.0
18	G	2.843382E-06 0.0	-2.272007E-04 0.0	-2.330878E-02 0.0	-4.051833E-06 0.0	-2.107554E-05 0.0	7.130619E-06 0.0
19	G	-8.379902E-05 0.0	-3.702281E-05 0.0	-2.231085E-02 0.0	-3.197886E-07 0.0	-7.413507E-05 0.0	1.073782E-05 0.0
20	G	-2.510604E-04 0.0	2.268255E-04 0.0	-2.002459E-02 0.0	4.619299E-06 0.0	-1.437334E-04 0.0	1.469436E-05 0.0
21	G	-5.231038E-04 0.0	5.680122E-04 0.0	-1.604917E-02 0.0	1.098687E-05 0.0	-2.349665E-04 0.0	1.882315E-05 0.0
22	G	-9.238772E-04 0.0	9.915794E-04 0.0	-1.002822E-02 0.0	1.906521E-05 0.0	-3.385027E-04 0.0	2.347003E-05 0.0
23	G	-1.470300E-03 0.0	1.510291E-03 0.0	-1.677037E-03 0.0	3.034136E-05 0.0	-4.567634E-04 0.0	2.911233E-05 0.0
24	G	-2.165156E-03 0.0	2.146461E-03 0.0	-9.089150E-03 0.0	4.714845E-05 0.0	-5.870916E-04 0.0	3.630105E-05 0.0

PILOT SEAT RESPONSE TO 1000 LB Z/REV VERT HUB SHEAR
FREQUENCY = 1.080000E+01

C O M P L E X D I S P L A C E M E N T V E C T O R
(REAL/IMAGINARY)

POINT ID.	TYPE	T1	T2	T3	R1	R2	R3
26	G	-1.117396E-02 0.0	1.965181E-03 0.0	1.840866E-02 0.0	1.127584E-04 0.0	-5.869644E-04 0.0	9.547995E-05 0.0
27	G	-1.620716E-02 0.0	1.832145E-03 0.0	2.361178E-02 0.0	1.622681E-04 0.0	-6.079494E-04 0.0	1.400797E-04 0.0
28	G	-2.146809E-02 0.0	1.666112E-03 0.0	2.907395E-02 0.0	2.214033E-04 0.0	-6.265466E-04 0.0	1.934432E-04 0.0
29	G	-2.669807E-02 0.0	1.464866E-03 0.0	3.466991E-02 0.0	2.929114E-04 0.0	-6.396722E-04 0.0	2.584504E-04 0.0
30	G	-3.241684E-02 0.0	1.219792E-03 0.0	4.037144E-02 0.0	3.767423E-04 0.0	-6.501069E-04 0.0	3.345830E-04 0.0
31	G	-3.816655E-02 0.0	-4.989358E-04 0.0	4.378986E-02 0.0	4.156823E-04 0.0	-6.532557E-04 0.0	3.698836E-04 0.0
32	G	-4.082972E-02 0.0	-4.989377E-04 0.0	4.678277E-02 0.0	4.777317E-04 0.0	-6.532557E-04 0.0	4.240985E-04 0.0
33	G	-4.431936E-02 0.0	-4.989391E-04 0.0	5.072388E-02 0.0	5.178971E-04 0.0	-6.532557E-04 0.0	5.465662E-04 0.0
34	G	1.165710E-03 0.0	-4.463129E-05 0.0	-1.148170E-02 0.0	-1.253787E-05 0.0	1.121787E-04 0.0	-3.951713E-06 0.0
35	G	1.120495E-03 0.0	-4.449481E-05 0.0	-1.133553E-02 0.0	-1.298460E-05 0.0	1.120947E-04 0.0	-3.955556E-06 0.0
36	G	1.088434E-03 0.0	-4.488064E-05 0.0	-1.123883E-02 0.0	-1.373882E-05 0.0	1.119525E-04 0.0	-3.967531E-06 0.0
37	G	1.060906E-03 0.0	-4.580986E-05 0.0	-1.116608E-02 0.0	-1.491748E-05 0.0	1.117308E-04 0.0	-3.977905E-06 0.0
38	G	1.217054E-03 0.0	-4.580931E-05 0.0	-1.194101E-02 0.0	-2.574705E-05 0.0	1.117561E-04 0.0	-4.168935E-06 0.0
39	G	1.332711E-03 0.0	-3.758240E-05 0.0	-1.245458E-02 0.0	-2.711693E-05 0.0	1.120140E-04 0.0	-4.184752E-06 0.0
40	G	1.466774E-03 0.0	-2.729098E-05 0.0	-1.306318E-02 0.0	-2.800898E-05 0.0	1.121824E-04 0.0	-4.202487E-06 0.0
41	G	1.654888E-03 0.0	-1.216544E-05 0.0	-1.392617E-02 0.0	-2.855[illegible]E-05 0.0	1.122644E-04 0.0	-4.208870E-06 0.0
42	G	3.062717E-03 0.0	3.175149E-04 0.0	-1.099291E-02 0.0	-2.000533E-05 0.0	1.115734E-04 0.0	-4.062023E-06 0.0
43	G	3.163252E-03 0.0	3.175149E-04 0.0	-1.148804E-02 0.0	-2.000533E-05 0.0	1.115734E-04 0.0	-4.062023E-06 0.0
44	G	3.062717E-03 0.0	2.229044E-04 0.0	-1.342298E-02 0.0	-2.000533E-05 0.0	1.115734E-04 0.0	-4.062023E-06 0.0
45	G	3.163252E-03 0.0	2.229044E-04 0.0	-1.391811E-02 0.0	-2.000533E-05 0.0	1.115734E-04 0.0	-4.062023E-06 0.0
46	G	3.117964E-03 0.0	2.177517E-04 0.0	-1.396072E-02 0.0	-2.000533E-05 0.0	1.115734E-04 0.0	-4.062023E-06 0.0
47	G	3.231415E-03 0.0	3.302386E-04 0.0	-1.234166E-02 0.0	-5.024988E-06 0.0	-9.323143E-05 0.0	-4.099636E-06 0.0
48	G	3.343921E-03 0.0	3.302386E-04 0.0	-1.284603E-02 0.0	-5.024988E-06 0.0	-9.323143E-05 0.0	-4.099636E-06 0.0
49	G	3.231415E-03 0.0	2.404987E-04 0.0	-1.031106E-02 0.0	-5.024988E-06 0.0	-9.323143E-05 0.0	-4.099636E-06 0.0

PILOT SEAT RESPONSE TO 1000 LB 2/REV VERT HUB SHEAR
FREQUENCY # 1.000000E+01

C O M P L E X D I S P L A C E M E N T V E C T O R
%REAL/IMAGINARY%

POINT ID.	TYPE	T1	T2	T3	R1	R2	R3
49	G	3.342921E-03 0.0	2.409487E-04 0.0	-1.043545E-02 0.0	-5.024988E-06 0.0	-9.323143E-05 0.0	-4.099636E-06 0.0
50	G	3.262186E-03 0.0	2.295517E-04 0.0	-1.011408E-02 0.0	-5.024988E-06 0.0	-9.323143E-05 0.0	-4.099636E-06 0.0
51	G	2.701357E-03 0.0	3.203021E-04 0.0	-1.146594E-02 0.0	-5.024988E-06 0.0	-9.323143E-05 0.0	-4.099636E-06 0.0
52	G	3.316684E-03 0.0	2.871372E-04 0.0	-1.146594E-02 0.0	-5.024988E-06 0.0	-9.323143E-05 0.0	-4.099636E-06 0.0
53	G	1.377471E-03 0.0	3.916568E-04 0.0	-1.129531E-02 0.0	3.405797E-07 0.0	-6.145172E-05 0.0	-4.099636E-06 0.0
54	G	6.455895E-04 0.0	3.302987E-04 0.0	-1.114966E-02 0.0	6.638505E-06 0.0	-2.703117E-05 0.0	-4.099636E-06 0.0
55	G	4.874486E-04 0.0	-9.968260E-05 0.0	-1.081774E-02 0.0	1.365370E-05 0.0	7.273181E-06 0.0	-4.099636E-06 0.0
60	G	4.118551E-03 0.0	1.304774E-04 0.0	-1.811508E-02 0.0	-1.511648E-05 0.0	1.134100E-04 0.0	-1.504861E-06 0.0

*** USER WARNING MESSAGE 2354.
GPFDR MODULE IS UNABLE TO CONTINUE AND HAS BEEN TERMINATED DUE TO ERROR MESSAGE PRINTED ABOVE OR BELOW THIS MESSAGE.
THIS ERROR OCCURRED IN GPFDR CODE WHERE THE VARIABLE -NERROR- WAS SET # 20

PILOT SEAT RESPONSE TO 1000 LB 2/REV VERT HUB SHEAR

*** SYSTEM WARNING MESSAGE 3002
EOF ENCOUNTERED WHILE READING DATA SET SCRATCH3XFILE 303< IN SUBROUTINE GPFDR

PILOT SEAT RESPONSE TO 1000 LB 2/REV VERT HUB SHEAR

E L E M E N T S T R A I N E N E R G I E S

ELEMENT-TYPE # BAR * TOTAL FOR ALL TYPES # 4.366282 3E+00

ELEMENT-ID	STRAIN-ENERGY	PERCENT OF TOTAL *
12	5.900181E-06	0.0001
23	3.840236E-06	0.0001
34	2.535060E-06	0.0001
46	1.185271E-04	0.0027
67	7.495412E-05	0.0017
78	1.392690E-03	0.0319
89	2.341652E-03	0.0536
910	2.443716E-03	0.0559
1011	4.364190E-02	0.9991
1112	1.901398E-02	0.4353
1213	3.301403E-02	0.7558
1237	1.605901E-03	0.0368
1314	3.453401E-02	0.7906
1415	1.666654E-01	3.8154
1516	1.980183E-01	4.5331
1617	2.428970E-01	5.5605
1718	2.659355E-01	6.0879
1819	3.322464E-01	7.6059
1920	4.058198E-01	9.2901
2021	4.809276E-01	11.0095
2122	4.783912E-01	10.9515
2223	4.627764E-01	10.5940
2324	3.531976E-01	8.0855
2425	6.755239E-02	1.5464
2526	5.046421E-02	1.1552
2627	4.159051E-02	0.9521
2728	3.386378E-02	0.7752
2829	3.132105E-02	0.7170
2930	1.091248E-02	0.2498
3031	7.981073E-03	0.1827
3132	1.202663E-02	0.2753
3334	1.535723E-06	0.0000
3435	3.553541E-05	0.0008
3536	1.174821E-04	0.0027
3612	1.270350E-03	0.0291
3738	1.675325E-04	0.0038
3839	5.456746E-05	0.0012
3940	3.991257E-06	0.0001
5112	9.002715E-02	2.0609
5253	7.428759E-02	1.7006
5354	6.638360E-02	1.5197
5455	1.465602E-01	3.3561

PILOT SEAT RESPONSE TO 1000 LB 2/REV VERT HUB SHEAR

E L E M E N T S T R A I N E N E R G I E S

ELEMENT-TYPE # ELAS1 * TOTAL FOR ALL TYPES # 4.3682823E+00

ELEMENT-ID	STRAIN-ENERGY	PERCENT OF TOTAL *
41461	4.112961E-04	0.0094
41462	2.245739E-06	0.0001
41463	4.190624E-03	0.0959
42471	4.157592E-04	0.0095
42472	2.245739E-06	0.0001
42473	2.164913E-03	0.0496
43481	4.112961E-04	0.0094
43482	1.965862E-06	0.0000
43483	2.192342E-02	0.5019
44491	4.157592E-04	0.0095
44492	1.965862E-06	0.0000
44493	2.764633E-02	0.6329
45503	1.510120E-01	3.4570

*** USER WARNING MESSAGE 2354,
GPFDR MODULE IS UNABLE TO CONTINUE AND HAS BEEN TERMINATED DUE TO ERROR MESSAGE PRINTED ABOVE OR BELOW THIS MESSAGE.
THIS ERROR OCCURRED IN GPFDR CODE WHERE THE VARIABLE -NERROR- WAS SET # 20

*** SYSTEM WARNING MESSAGE 3002
EOF ENCOUNTERED WHILE READING DATA SET SCRATCH3%FILE 303< IN SUBROUTINE GPFDR

PILOT SEAT RESPONSE TO 1000 LB 2/REV VERT HUB SHEAR

E L E M E N T S T R A I N E N E R G I E S

ELEMENT-TYPE # BAR * TOTAL FOR ALL TYPES # 4.2046100E+00

ELEMENT-ID	STRAIN-ENERGY	PERCENT OF TOTAL
12	-4.921822E-07	-0.0000
23	2.638168E-06	0.0001
34	-9.079613E-07	-0.0000
46	4.671328E-05	0.0011
67	2.231710E-04	0.0053
78	2.389228E-03	0.0568
89	3.805750E-03	0.0833
910	2.878208E-03	0.0684
1011	5.114004E-02	1.2148
1112	2.102199E-02	0.4994
1213	3.813657E-02	0.9059
1237	1.571460E-03	0.0373
1314	2.991120E-02	0.7105
1415	1.513309E-01	3.5949
1516	1.835586E-01	4.3605
1617	2.271718E-01	5.3965
1718	2.503878E-01	5.9480
1819	3.149040E-01	7.4806
1920	3.867560E-01	9.1874
2021	4.603697E-01	10.9362
2122	4.596977E-01	10.9202
2223	4.463311E-01	10.6027
2324	3.420211E-01	8.1248
2425	6.544316E-02	1.5546
2526	4.938817E-02	1.1732
2627	3.952727E-02	0.9390
2728	3.290632E-02	0.7817
2829	3.005898E-02	0.7141
2930	1.021770E-02	0.2427
3031	7.778548E-03	0.1848
3132	1.171866E-02	0.2784
3334	1.257398E-06	0.0000
3435	3.488512E-05	0.0008
3536	1.199205E-04	0.0028
3612	1.234347E-03	0.0293
3738	1.708630E-04	0.0041
3839	5.777416E-05	0.0014
3940	1.440337E-06	0.0000
5112	9.091341E-02	2.1597
5253	7.537621E-02	1.7906
5354	6.732237E-02	1.5993
5455	1.478415E-01	3.5049

PILOT SEAT RESPONSE TO 1000 LB 2/REV VERT HUB SHEAR

ELEMENT STRAIN ENERGIES

ELEMENT-TYPE # ELAS1 * TOTAL FOR ALL TYPES # 4.2096100E+00

ELEMENT-ID	STRAIN-ENERGY	PERCENT OF TOTAL *
41461	4.003979E-04	0.0095
41462	2.278618E-06	0.0001
41463	4.093051E-03	0.0972
42471	4.048273E-04	0.0096
42472	2.278618E-06	0.0001
42473	2.152028E-03	0.0511
43481	4.003979E-04	0.0095
43482	1.992921E-06	0.0000
43483	2.178884E-02	0.5176
44491	4.048273E-04	0.0096
44492	1.992921E-06	0.0000
44493	2.729011E-02	0.6483
45503	1.495064E-01	3.5516

SYMBOLS

A	Element cross-sectional area
C	Viscous damping matrix
E	Modulus of elasticity
F	Applied force
G	Complex receptance matrix
I	Element area moment of inertia
K	Stiffness matrix
k	Scalar spring
M	Mass matrix
m	Scalar mass
S	Stiffness ratio
SE	Strain energy
t	Time
x	Structural displacement response vector
Z	Pilot's seat vertical displacement response
δ	Element displacement response vector
ω	Circular frequency of the applied forces
ϕ	Element natural frequency mode shape (eigenvector)
ζ	Element structural damping coefficient

Subscripts

b	Baseline
e	Element
I	Imaginary component of response

$_j$ jth element

m At minimum response

n At resonance

R Real component of response

Superscripts

T Matrix transpose

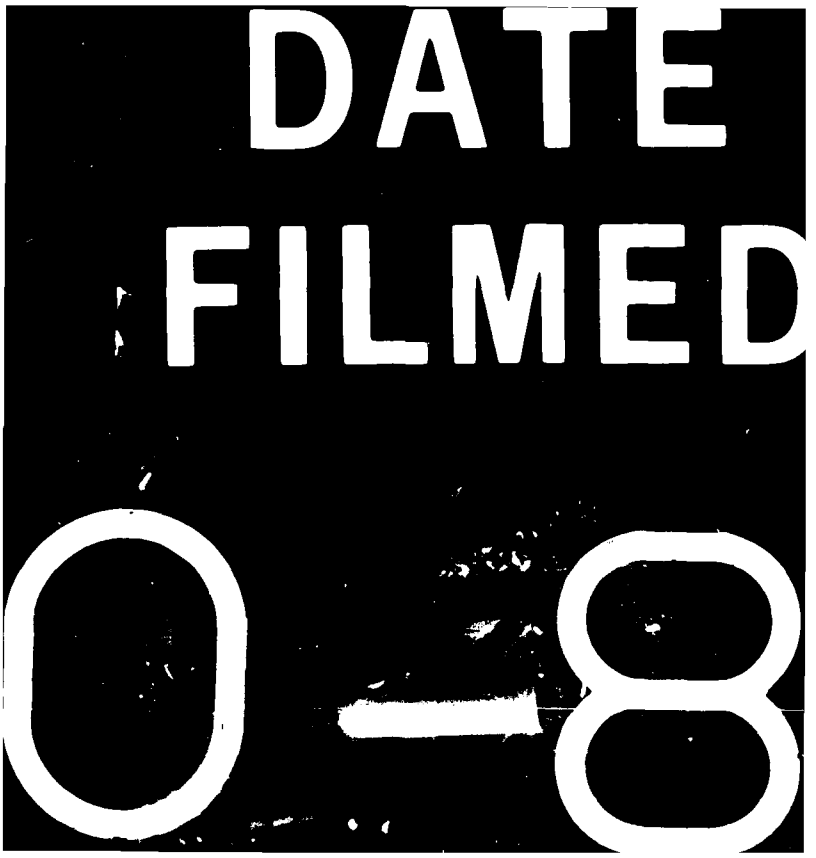
DATE
FILMED
0-8